Title: Planarian dorsoventral Netrins organize a muscle midline signaling center and regulate blastema formation

Authors and Affiliations:

Erik G. Schad[1]

Christian P. Petersen*[1,2]

1-Department of Molecular Biosciences, Northwestern University, Evanston, IL 60208

2-Robert Lurie Comprehensive Cancer Center, Northwestern University, Evanston IL 60208

*-corresponding author, christian-p-petersen@northwestern.edu

Abstract

Integration of positional information across body axes is likely critical for whole-body regeneration to define the territories of missing tissue in three dimensions with fidelity. The body-wall musculature in planarians expresses patterning factors regulating the anteroposterior, dorsoventral, and mediolateral axes, but how this information coordinates is not fully understood. Using analysis of scRNAseq data, we identify *pitx* and *islet* transcription factors as regulators of a dorsal muscle midline signaling center expressing a the BMP/Activin decoy receptor *bambi-2*. Dorsal midline cells are comprised of longitudinal muscle and are required for blastema formation in fragments lacking a pre-existing midline. In laterally amputated animals regenerating an entirely new midline, *bambi-2*+ cells are initially formed at the dorsal-most region of the excised tissue fragment, then dynamically spread and ultimately reset to restore bilateral symmetry, rather than forming at the initial geometric mediolateral midpoint. We further identify a system of dorsoventral Netrin and Netrin receptor signals expressed from body-wall muscle that control midline identity and blastema morphology. Ventral and laterally expressed *netrins -1, -4,* and *-5* signal via dorsally-enriched netrin repulsion receptors *unc-5C, unc-5E,* and *dcc-2*, which together limit mediolateral spread of *bambi-2*+ dorsal midline muscle and enable muscle targeting across the midline. Our results suggest a model in which ventral determinants dictate mediolateral information important for blastema patterning.

Introduction

Whole body regeneration involves tissue restoration from a variety of possible truncations to axis content after amputation. Species of planarians, acoels, and cnidarians exemplify these abilities, as they are able to regenerate essentially entirely new animals after even severe injuries such as decapitation (Reddien, 2018; Vogg et al., 2019; Srivastava, 2022). The nature of robust positional information is therefore important to understand how extreme regenerative ability is possible. The information systems controlling regenerative ability across each body axis have often been considered separately, but surgical injuries also frequently damage more than one orthogonal body axis. How overall patterning across axes is accomplished

53 is incompletely understood and may be important for understanding how regenerative organisms correctly
54 match blastema specification to the identity and content of pre-existing tissue

55 Flatworm planarians can regenerate from nearly any type of surgical injury to restore axis content
56 along their anteroposterior (AP), dorsoventral (DV), and mediolateral (ML) axes. A system of posterior
57 Wnts and anterior Wnt inhibitors are expressed in gradients along the AP axis, and inhibition of canonical
58 Wnt signaling results in ectopic head regeneration while over-activation due to inhibition of anti-Wnt
59 factors results in ectopic tail regeneration (Gurley et al., 2008; Iglesias et al., 2008; Petersen and Reddien,
60 2008; Petersen and Reddien, 2009; Gurley et al., 2010; Petersen and Reddien, 2011; Owen et al., 2015;
61 Reuter et al., 2015; Stuckemann et al., 2017). In addition, two Wnt/FGFRL systems control head and trunk
62 regionalization in conjunction with Disheveled and Src signals (Cebria et al., 2002; Almuedo-Castillo et
63 al., 2011; Lander and Petersen, 2016; Scimone et al., 2016; Bonar et al., 2022). By contrast, the dorso-
64 ventral (DV) axis is controlled through dorsal *bmp4* signals and ventral *admp*, which signal in a negative
65 feedback loop (Molina et al., 2007; Orii and Watanabe, 2007; Reddien et al., 2007; Gavino and Reddien,
66 2011). Finally, medio-lateral axis patterning is regulated by medially expressed *slit* which opposes laterally
67 expressed *wnt5* (Cebria et al., 2007; Gurley et al., 2010).

68 The major signals specifying AP, DV, and ML pattern in planarians are expressed from
69 subepidermally located muscle body-wall cells that surround the inner parenchymal region containing the
70 neoblast planarian stem cells (Witchley et al., 2013). Neoblasts are pluripotent and generate all planarian
71 adult differentiated cells, thus underlying the animal's ability to replace diverse missing tissues and undergo
72 perpetual tissue homeostasis in the absence of injry (Wagner et al., 2011; Reddien, 2018; Zeng et al., 2018).
73 Planarian muscle cells are mononucleated and project contractile fibers across several orientations
74 (longitudinal, diagonal, circular, and dorsoventral orientations) to form a meshwork plexus (Witchley et al.,
75 2013; Cebria, 2016). The majority of patterning factors controlling regionalization are expressed from
76 multiple muscle subtypes (Scimone et al., 2017). However, analysis of cell fate transcription factors
77 required for producing individual muscle subtypes found that some patterning genes have expression
78 restricted to muscle oriented in particular directions. For example, injury triggers expression of the Wnt

79 inhibitor *notum* and the Activin pathway modulator *follistatin*, important for wound polarization and
80 outgrowth (Petersen and Reddien, 2011; Gavino et al., 2013; Roberts-Galbraith and Newmark, 2013;
81 Tewari et al., 2018), and inhibition of the longitudinal muscle fate transcription factor *myoD* prevents their
82 expression and leads to failed regeneration (Scimone et al., 2017). Likewise, circular muscle requires *nkx1.1*
83 for its production, selectively expresses *activin-2* involved in polarity determination (Cloutier et al., 2021),
84 and inhibition of *nkx1.1* leads to splitting the anterior pole and formation of split-axis animals (Scimone et
85 al., 2017). In addition, medial dorsoventral muscle controlled by *foxF1* and *gata4/5/6-2* factors is a source
86 of *slit* (Scimone et al., 2018). However, little is known about how the muscle system becomes organized
87 and how axis patterning systems communicate with each other to result in a restoration of form following
88 injury.

89 Prior studies have suggested the existence of communication across the body axes. The master
90 regulator of posterior identity *wnt1* is required for posterior regeneration and is expressed selectively in the
91 posterior along the dorsal midline (Petersen and Reddien, 2009; Gurley et al., 2010). *wnt1* is co-expressed
92 in a posterior subpopulation of dorsal midline (DM) muscle cells which express the previously unannotated
93 gene *dd23400* and extend across the majority of the AP axis (Fincher et al., 2018; Schad and Petersen,
94 2020). Overactivation of *wnt1* in *dd23400+* DM muscle cells through inhibition of *mob4* or *striatin*
95 components of the STRIPAK complex results in the expansion of posterior tissue in homeostasis and
96 regeneration, suggesting that regulation of DM muscle cells is important for body patterning (Schad and
97 Petersen, 2020). Additionally, the correct placement of the *notum+* anterior pole at the mediolateral and
98 dorsoventral midpoint is dependent on mediolateral components *wnt5* and *slit*, as well as the dorsoventral
99 regulator *bmp4* (Oderberg et al., 2017). These observations suggest that patterning information may
100 communicate across orthogonal axes and also the importance of the dorsal midline in regeneration.
101 However, the roles for dorsal midline muscle cells in regeneration are not fully understood.

102 In order to understand how midline cells contribute to regeneration, we analyzed single-cell
103 RNAseq data to identify factors expressed in midline muscle. This approach identified a set of transcription
104 factors required for DM muscle identity. We found that factors required for DM formation were also

105 required for lateral regeneration, suggesting the importance of these cells in facilitating outgrowth during
106 formation of a new mediolateral axis through regeneration. Furthermore, by tracking expression of midline
107 markers, we find that the re-establishment of dorsal midline during lateral regeneration proceeds from the
108 wound edge rather than the mediolateral center of the fragment. Using candidate approaches, analysis of
109 scRNAseq data, and functional analysis, we furthermore implicate Netrin related signals as regulators
110 restricting the domain of DM cells. Netrins are a class of secreted proteins known for their role in axonal
111 guidance (Hedgecock et al., 1990; Ishii et al., 1992; Kennedy et al., 1994; Serafini et al., 1994), and play a
112 role in axon growth and regeneration in planarians (Cebria and Newmark, 2005). Other known roles for
113 Netrins include cell survival (Mehlen et al., 1998; Llambi et al., 2001), organ morphogenesis (Dalvin et al.,
114 2003; De Breuck et al., 2003; Srinivasan et al., 2003; Yebra et al., 2003; Liu et al., 2004), and myotube
115 formation (Kang et al., 2004). In order to transduce their signals, Netrins bind a variety of targets including
116 UNC-5 (Hedgecock et al., 1990) and DCC (Chan et al., 1996; Keino-Masu et al., 1996; Kolodziej et al.,
117 1996; Fazeli et al., 1997). There are five genes encoding Netrins in planarians, all of which have prominent
118 expression in muscle cells and are regionally expressed across the ML and DV axes (Cebria and Newmark,
119 2005; Scimone et al., 2017; Fincher et al., 2018). In planarians, Netrin receptors (five UNC-5s, two DCCs)
120 are expressed widely, including in muscle cells (Fincher et al., 2018). Because Netrins and their receptors
121 are expressed in muscle cells regionally across the ML or DV axes like other genes controlling patterning
122 in planarians, we hypothesized that Netrins organize key features across these body axes, in particular, DM
123 muscle cells.
124
125 **Results**
126 *dd23400/bambi-2+* dorsal midline muscle cells are important for lateral blastema outgrowth
127 To identify factors important for DM muscle, we sought genes expressed in this cell population. Prior
128 single-cell RNA seq analysis identified a gene *dd23400* expressed exclusively on the dorsal midline from
129 muscle cells. This gene was originally identified without discernable sequence similarity to other proteins
130 (Fincher et al., 2018). However, we noticed that PSI-blast of *dd23400* recovered several homologs of a

131 family of Bmp/Activin membrane-bound inhibitors (Figure S1) whose members possess extracellular ActR
132 domains, lack intracellular activation domains, and may therefore function as decoy receptors (Onichtchouk
133 et al., 1999). SMART domain analysis weakly identified an ActR domain in *dd23400* and also a
134 transmembrane domain. Using maximum-likelihood phylogenies, *dd23400* placed with strong support
135 within a clade of bilaterian BAMBI homologs separate from BMPR1 receptors, and so we named the gene
136 *bambi-2*.

137 To examine the role of DM muscle cells in regeneration, we attempted to uncover factors required
138 for their production. We first re-examined a prior whole-animal single-cell RNAseq atlas generated by
139 DropSeq to search for factors expressed in *bambi-2*+ muscle cells (Fincher et al., 2018). Because *bambi-2*
140 has relatively weak expression, we searched for cells co-expressing *bambi-2* and the midline factor *slit,* and
141 compared these to bulk muscle cells using the scde package for differential gene expression profiling from
142 single-cell RNAseq data (Kharchenko et al., 2014). The resulting analysis identified several genes
143 putatively enriched for expression in *bambi2*+ midline muscle cells, including *pitx, bmp, msx, myoD, fgfr4,*
144 *delta-like, TM211, nephrin, unc5-C,* and *fgfr4* (Figure 1A, Table S1). A prior analysis using Smart-Seq to
145 find transcriptome information for *wnt1*+ cells identified enriched expression (log fold-change > 2) in these
146 cells for *pitx, wif, nephrin, msx, fgfr4, bmp, myoD, unc5-C, TM211, delta-like,* and *bambi-2* (Li et al., 2019).
147 As a further test of midline enrichment, we used performed colorimetric whole-mount in situ hybridizations
148 on several candidates to examine whether which had midline expression. We found midline-related
149 expression for 11 out of 15 factors tested, with the remaining 4 lacking detection in the assay (Figure 1A,
150 Figure S1). The transcription factor *pitx* was identified previously as important for expression of *wnt1*
151 (Currie and Pearson, 2013; März et al., 2013), a master regulator of posterior formation expressed from the
152 posterior dorsal midline (Petersen and Reddien, 2009; Gurley et al., 2010). Posterior *wnt1* was subsequently
153 shown to be co-expressed in a posterior subset of *23400/bambi-2*+ dorsal midline muscle cells (Schad and
154 Petersen, 2020). We used FISH to verify that *pitx* has expression along the dorsal midline (Figure 1B). We
155 further reasoned that other factors required for *wnt1* expression might also have expression on the dorsal
156 midline. The transcription factor *islet* is required for expression of *wnt1* (Hayashi et al., 2011) and although

157 our analysis of a DropSeq atlas did not identify enrichment for this gene in midline muscle, a prior analysis
158 using SmartSeq found enrichment for *islet* expression in *wnt1+* posterior midline cells. Using FISH, we
159 found *ilset* is expressed more broadly than *pitx,* but including dorsal midline cells in the anterior and
160 posterior of the animal (Figure 1B).

161 We observed that in addition to expression on the dorsal midline in the posterior, *islet* and *pitx* are
162 also expressed on the DM in the anterior (Figure 1B), so we reasoned that they could be required for all
163 *bambi-2+* cells. We performed RNAi of *islet* and *pitx,* and found a nearly complete loss of *bambi-2*
164 expression (Figure 1C). *bambi-2+* DM muscle cells may additionally be specified by transcription factors
165 required for other muscle cell subsets. The *myoD* transcription factor is required for longitudinal muscle
166 throughout the body (Scimone et al., 2017), was recovered by scRNAseq analysis as enriched in *bambi-2+*
167 midline cells and its expression domain includes a midline-enriched region expression pattern (Figure 1A),
168 so we tested whether *myoD* inhibition would impact *bambi-2* dorsal muscle expression. RNAi of *myoD*,
169 but not the *nkx1.1* transcription factor required for circular muscle, caused a loss of *bambi-2* expression,
170 suggesting that *bambi-2+* DM muscle cells are likely a subset of longitudinal muscle (Figure 1B). We
171 further sought to test whether *pitx* and *islet* were required only for expression of *bambi-2* or important for
172 expression of other markers of dorsal midline. *dachsous* has midline expression (Vu et al., 2019) and was
173 weakly enriched for expression in midline muscle by the scde analysis (Table S1, upper bound enrichment
174 of 3.10). *pitx* or *islet* RNAi resulted in a loss of *dachsous* expression (Figure 1D). Furthermore, a homolog
175 of *Wnt inhibitory factor (wif)* (Hsieh et al., 1999), a homolog of Drosophila *shifted* (Glise et al., 2005), was
176 recovered as strongly enriched in *bambi-2+* muscle cells from the single-cell RNAseq analysis (Figure 1A,
177 upper bound enrichment 10.92). FISH analysis revealed *wif* to be expressed weakly along the dorsal
178 midline, and inhibition of *pitx* or *islet* similarly reduced *wif* expression. Therefore, *pitx* and *islet* are
179 important for expression of several markers of dorsal midline muscle. We also used the additional markers
180 of midline muscle to examine the consequences of *bambi-2* inhibition on these cells. *bambi-2(RNAi)*
181 animals appeared phenotypically normal and did not fail to express midline *dachsous* or *wif* (Figure 1C-D).
182 Therefore, *bambi-2* is a marker of dorsal midline but likely not critical for its formation.

183 *islet* and *pitx* are known to be required for posterior regeneration (Figure 2A), likely through their
184 requirement for *wnt1* expression (Hayashi et al., 2011; Currie and Pearson, 2013; Marz et al., 2013).
185 However, our findings that these genes are required more broadly for *bambi-2*+ dorsal midline prompted
186 us to examine whether they might also be required for regeneration in other contexts that involve generation
187 of new midline tissue. To further examine the role of DM muscle cells in regeneration, we wounded animals
188 to create lateral regenerating fragments lacking midline following *islet* or *pitx* inhibition. Both *islet(RNAi)*
189 and *pitx(RNAi)* animals were defective in lateral blastema outgrowth compared to controls (Figure 2B). In
190 both cases, lateral fragments were unable to regenerate a *slit*+ midline, but were able to establish the lateral
191 edge as measured by *laminB* expression (Figure 2C). From these results, we conclude that *bambi-2*+ DM
192 muscle cells are important for blastema outgrowth but not re-establishment of lateral identity during
193 mediolateral regeneration.
194 Given the requirement of *pitx* and *islet* in the formation of a lateral blastema, we examined how
195 lateral regeneration normally accomplishes the re-establishment of midline tissue. Thin lateral fragments
196 initially lack a midline after amputation, yet regenerate into an animal in which bilateral symmetry is
197 ultimately restored. One possible mechanism to drive this process could be that such fragments would
198 define a new midline at the geometric midpoint of the amputated tissue, thereby preserving mediolateral
199 symmetry throughout regeneration. By contrast, through a FISH time-series analysis, we found that *bambi-*
200 *2* expression appeared by 24 hours at the wound edge at a location furthest from the existing lateral-most
201 domain (Figure 3). Over time, this expression domain expanded and reached a point of largest mediolateral
202 spread by 72 hours, followed by restriction to a location between the pre-existing tissue and growing
203 blastema. Therefore, lateral regeneration does not immediately reassign bilateral symmetry based on
204 fragment geometry. Instead, *bambi-2*+ cells appear at the dorsal-most position remaining in the fragment,
205 followed by subsequent expansion of domain identity and ultimately bilateral resolution.
206
207 *Netrins from ventral/medial muscle domains coordinate to instruct blastema outgrowth shape*

208 These observations suggested that inputs from dorsoventral signals could be important for
209 establishing the *bambi-2+* expression domain. We noticed that one of the genes enriched in midline muscle
210 expression from the scRNAseq analysis (*unc5*-C) belonged to the Netrin signaling pathway, suggesting a
211 possible role for this pathway in DM muscle function. Netrins are secreted proteins that provide guidance
212 cues for migratory cells (Hedgecock et al., 1990; Ishii et al., 1992) and can signal to receiving cells across
213 long ranges (Colavita and Culotti, 1998; Hong et al., 1999; Keleman and Dickson, 2001; Finci et al., 2014;
214 Boyer and Gupton, 2018). The planarian genome contains five genes encoding Netrin proteins, each
215 expressed in muscle cells (Figure 4A-C, Figure S2) (Fincher et al., 2018), while *netrin-1* and *netrin-2* are
216 also expressed in neurons (Cebria and Newmark, 2005; Scimone et al., 2017). Planarian Netrins are
217 expressed in a series of ML and DV domains (Figure 4A). *netrin-1* and *netrin-3* are coexpressed in
218 *collagen+* muscle cells on the lateral edge of the animal, while *netrin-2* and *netrin-5* are expressed in medial
219 muscle cells on the ventral side (Figure 4A). *netrin-4* is expressed across the ventral side of the animal
220 (Figure 4A). Sections of animals co-stained with each Netrin and the muscle marker *collagen* showed that
221 Netrins are expressed in several ventral/medial domains within muscle. Netrins in cell guidance and their
222 graded expression in muscle cells on the ML axis, we hypothesized that Netrins play a role in organizing
223 the DM muscle domain. Netrins signal through binding receptors, and the planarian genome encodes five
224 putative UNC-5 receptors, and two DCC receptors (Scimone et al., 2020). Each of these receptors is
225 expressed broadly, but also has graded expression in muscle cells (Fincher et al., 2018) (Figure 4B-C,
226 Figure S2). *unc5-A,-B,-D* and *dcc-1/net-R* are expressed on the lateral edge of the animal, while *unc5-C,-E*
227 and *dcc-2* have prominent expression in dorsal medial *collagen+* muscle cells (Figure 4B-C). In summary,
228 Netrins are expressed in either lateral (*netrin-1,-3),* ventral-medial (*netrin 2,-5*), or broad ventral (*netrin-4*)
229 domains, while putative receptors are expressed in lateral (*unc5-A,-B,-D* and *dcc-1/net-R*) or dorso-medial
230 (*unc5-C,-E* and *dcc-2*) domains (Figure 4D).

231 To investigate the role of Netrins during regeneration we inhibited each Netrin using RNAi. We
232 first inhibited each Netrin individually, resulting in no overt phenotypes of dysfunction in either anterior or
233 posterior regeneration (Figure 5A). We reasoned that Netrins could function redundantly, and so we

234 inhibited all five planarian Netrins through combined RNAi, and verified by qPCR for effective knockdown
235 (Figure S3). Inhibition of all Netrins simultaneously resulted in regeneration with midline defects of a
236 pointy blastema in the anterior (32/36 regenerating trunk fragments), and of indented blastemas in the
237 posterior (7/36) (Figure 5B). In addition, at a low frequency, inhibition of the five Netrins resulted in failed
238 anterior regeneration in amputated tail fragments (6/36) or failed posterior regeneration from amputated
239 head fragments (5/36 animals). We reasoned that these phenotypes were either due to inhibition of all
240 Netrins together or instead due to inhibition of subsets of Netrins. To test this hypothesis, we inhibited each
241 possible combination of two, three, or four Netrins, and scored animals for the penetrance and expressivity
242 of pointy blastema in anterior blastemas or indentations in posterior blastemas (Figure S4A-B). We found
243 that inhibition of all combinations of Netrins resulted in anterior pointy blastemas to varying degrees.
244 Inhibition conditions including RNAi of *netrin-4,-5* yielded the strongest effects on pointy blastemas,
245 followed by those including *netrin-1* and *netrin-2*. The laterally expressed *netrin-3* factor likely did not
246 contribute, because *netrin-1;-2;-3;-4;-5* RNAi yielded the same outcome as *netrin-1;-2;-4;-5* RNAi (Figure
247 S4A). Therefore, *netrin-1, -2 ,-4,* and *-5* contribute to normal anterior regeneration morphology.

248 A similar analysis of the indented blastema phenotype from posterior-facing wounds found a
249 distinct outcome. Whereas inhibition of all five Netrins simultaneously resulted in an indented blastema,
250 inhibition of most combinations of Netrins resulted in normal posterior regeneration. Inhibition of *netrin-*
251 *1, -4,* and *-5* increased the penetrance and expressivity of indentation over that from inhibition of all netrins,
252 indicating a particular importance for these three genes in enabling midline regeneration in the posterior
253 (Figure S4B). Consistent with this model, RNAi combinations excluding inhibition of any of these three
254 Netrins resulted in normal posterior regeneration, and co-inhibitions with *netrin-2* or *netrin-3* did not
255 strongly affect the outcome. Therefore, *netrin-1*, *netrin-4*, and *netrin-5* act together to ensure midline
256 regeneration in blastemas generating posterior tissue. In addition, these results suggest that the phenotypes
257 of pointy blastema and indented blastema from Netrin RNAi are partially separable because they involve
258 different subsets of netrins.

259 We also examined whether the low frequency of failed regeneration could be explained by lack of
260 injury-induced gene expression from muscle cells. However, *netrin-1;-2;-3;-4;-5(RNAi)* animals had
261 normal injury-induced expression of *notum* and *follistatin* (Figure S5). We suggest these phenotypes could
262 be reflective of a stronger expressivity of phenotypes in which normal blastema morphology is modified.
263 Nonetheless, these results suggest that Netrin inhibition does not result in failed responsiveness of
264 longitudinal muscle cells to injury (Scimone et al., 2017).

265 To further investigate the role of Netrins signaling in regeneration, we conducted RNAi
266 experiments to test for functions of the Netrin receptors. Inhibition of the receptors expressed in lateral
267 domains (*unc5-A,-B,-D* and *dcc-1/net-R*) appeared to result in normal regeneration, including when
268 inhibited in combination (Figure 5C). However, inhibition either *unc5-C, unc5-E*, or *dcc-2* caused
269 regeneration with indentations to posterior blastemas in all cases, and indentations to anterior regeneration
270 after *dcc-2* RNAi. Inhibition of both *unc5-E* and *unc5-C* or triple RNAi of *unc5-E;unc5-C;dcc-2* resulted
271 in more strongly expressive anterior and posterior blastema indentations. The indented posterior blastemas
272 were reminiscent of the posterior blastema morphology phenotypes after RNAi of *netrins-1, -4,* and *-5*,
273 suggesting these Netrins may signal through *unc5-E/unc5-C/dcc-2* receptors. Furthermore, while *netrin-1,*
274 *netrin-4* and *netrin-5* have expression from ventral and lateral muscle domains, *unc5-E* and *unc5-C* have
275 enrichment in a dorsal domain (Figure 4). These observations implicate a system of netrin ligands and netrin
276 receptors signaling across muscle domains in to control midline blastema morphology.

277

278 <u>Netrins act as repulsive signals to restrict the midline domain</u>

279 Based on the overt mediolateral defects in blastema formation after Netrin RNAi, we tested the
280 expression of ML and DV patterning factors in these animals. *netrin-1;-2;-3;-4;-5(RNAi)* animals displayed
281 an increase in *bambi-2* domain width, especially in the anterior (Figure 6A). Similarly, midline expression
282 of *slit* was also expanded in *netrin-1;-2;-3;-4;-5(RNAi)* animals, while laterally expressed *wnt5* was
283 unchanged (Figure 6A-C). Furthermore, *netrin-1;-2;-3;-4;-5(RNAi)* animals retained expression of dorsal
284 *bmp4* and ventral expression of *admp*, suggesting these animals did not undergo ventralization or

285 dorsalization (Figure 6A). Finally, *netrin-1;-2;-3;-4;-5(RNAi)* animals succeeded in expressing *wnt1+* at
286 the posterior pole and *notum* at the anterior pole, consistent with overall head and tail identity as intact in
287 spite of the blastema morphology defects (Figure 6A). We noted that although *notum* expression was
288 correctly located at the anterior pole, its expression was expanded over the pointy blastema compared to
289 controls. Prior studies suggest that a preexisting midline can determine the location of a newly regenerated
290 anterior pole (Oderberg et al., 2017), so perhaps the expanded midline domain in *netrin-1;-2;-3;-4;-5(RNAi)*
291 animals may cause formation of an expanded anterior pole. Together, these findings implicate Netrins
292 specifically in restricting dorsal midline identity. Based on these findings, we specifically tested for any
293 midline defects after inhibition of the Netrin receptors involved in midline formation. Simultaneous RNAi
294 of *unc5-C, unc5-E,* and *dcc-2* resulted in a similar expansion of the *bambi-2+* cell domain (Figure 4B-C).
295 Therefore, the phenotypes of dorsal midline expansion correlate with indented blastemas. Reception of
296 Netrins through receptor heterodimers of Unc5 and DCC family members are thought to signal repulsion
297 during axon guidance and cell migration (Lai Wing Sun et al., 2011). Furthermore, the *bambi-2+* dorsal
298 midline cells are located at the point furthest away from the sources of ventral and medial *netrin-1, netrin*
299 *-4* and *netrin-5* but within the dorsal domains of *unc5-E* and *unc5-C* expression. Therefore, we suggest that
300 the *bambi-2+* cells are restricted dorsally because of repulsive signaling between ventral/lateral *netrin-1,-*
301 *4,-5* to dorsally expressed Unc5 receptors *unc5-E* and *unc5-C* signaling through *dcc-2.*

302 The expression of Netrins within muscle cells led us to hypothesize that Netrins might control some
303 aspect of organization of the muscle fiber network important for blastema formation in regeneration. To
304 test this hypothesis, we inhibited all Netrins or Netrin receptors *unc5-E, unc5-C,* and *dcc-2*, and then used
305 immunofluorescence to label animals with a monoclonal antibody (6G10) that labels muscle cell fibers
306 (Ross et al., 2015) (Figure 6D). In *netrin-1,-2,-3,-4,-5(RNAi)* animals, muscle cell fibers were present in
307 anterior blastemas and appeared normal, although they tracked the overall pointed morphology. In the
308 posterior blastemas of *unc5-E;unc5-C;dcc-2* RNAi and *netrin-1,-2,-3,-4,-5(RNAi)* animals, circular muscle
309 fibers failed to appropriately cross the midline and instead projected dorsoventrally to individually encircle
310 and separate left and right blastema territories. *unc5-E;unc5-C;dcc-2* RNAi had a more severe defect of

311 indentation, and we also noticed such animals have a zone of disorganization immediately anterior to the
312 indentation along the midline, suggestive of a muscle remodeling process linked to indented tissue. We
313 conclude that a system of ventrally expressed Netrins and dorsally expressed Netrin Receptors are likely
314 not required for muscle fiber growth altogether, but instead restrict a domain of dorsal midline muscle
315 important for guiding muscle fiber growth across the midline and thereby contribute to regeneration with
316 normal bilateral symmetry.
317
318 **Discussion**
319 Whole-body regeneration requires the re-establishment of patterning across all major body axes.
320 Here, we identify processes important for generating, restricting, and using *bambi-2*+ dorsal midline muscle
321 in planarian regeneration. Inhibition of factors *pitx* and *islet* caused loss of midline expression of *bambi-2,*
322 *dachsous,* and *wif* and also prevented blastema outgrowth during lateral regeneration, suggesting the
323 importance of these cells in restoring mediolateral tissue distribution. We furthermore used *bambi-2*
324 expression as a probe to uncover the overall process of midline regeneration from fragments lacking a
325 midline. Rather than a potential mechanism of forming new midline from the center of an amputated lateral
326 fragment, planarians instead re-express *bambi-2* at the wound site whose location represents the dorsal-
327 most position of the injured animal. Subsequently, *bambi-2* expression expands and restricts to the interface
328 between new and old tissue, and differential growth over several weeks ultimately restores bilateral
329 symmetry (Figure 7A).
330 In addition, we describe the essential role of Netrin signaling in ML patterning during regeneration
331 in planarians (Figure 7B). *netrin-1,-2,-3,-4,-5* inhibition leads to an expansion of the *bambi-2*+ cell domain,
332 but does not alter lateral, DV, or AP markers. Netrins are known for their role in axonal growth (Hedgecock
333 et al., 1990; Ishii et al., 1992; Hamelin et al., 1993; Colavita and Culotti, 1998), including in planarians
334 (Cebria and Newmark, 2005), but Netrins can also act to guide myotube formation and other migrating cells
335 in murine development (Dalvin et al., 2003; De Breuck et al., 2003; Srinivasan et al., 2003; Yebra et al.,
336 2003; Kang et al., 2004; Liu et al., 2004), so it is plausible that Netrins may function to guide muscle cell

337 growth in planarians. Three putative Netrin receptors (*unc5-C, -E, dcc-2*) are expressed in dorso-medial
338 muscle cells, and their inhibition leads to an expansion of the *bambi-2+* cell domain. These results are
339 consistent with a model where Netrins act as repellants by binding to these receptors (Figure 7B). When
340 *netrin-1,-2,-3,-4,-5* are inhibited together, anterior blastemas form with a pointed morphology, with
341 expanded *notum+* anterior pole cells. Prior work determined that the midline instructs where the anterior
342 pole is placed in the anterior blastema (Oderberg et al., 2017), suggesting that the expanded dorsal muscle
343 domain from Netrin RNAi conditions may cause the regeneration of an excessively wide anterior pole, thus
344 generating pointed blastemas. Alternatively, it is possible that the pointy blastema phenotype represents a
345 loss of other outputs for Netrin activity. For example, Netrins can function as attractants in axon guidance
346 or migration, and this function is thought to occur via DCC/DCC receptor dimers rather than DCC/Unc5
347 dimers (Lai Wing Sun et al., 2011). No inhibition conditions of Netrin receptors phenocopied the pointy
348 blastema defect, and one possible explanation could be that due to the use of DCC in both repulsion and
349 attraction it is not possible to use RNAi to delineate only the process of attraction. Alternatively, perhaps
350 other receptors are responsible for the pointy blastema phenotype. Along these lines, we also did not find
351 blastema failure phenotypes through inhibition of Netrin receptors. However, our phenotypic analysis
352 identified shared functions in controlling the regeneration of midline tissue in the posterior as well as in
353 muscle targeting, for a subset of Netrins and Netrin receptors. RNAi of *netrin-1;-4;-5* or *unc5-C;unc5-*
354 *E;dcc-2* impacted the organization of the planarian musculature system, causing the newly made circular
355 muscle in regenerating blastemas to mistarget over the midline and instead forming separated domains that
356 grow into indented blastemas. Our results indicate that establishment of midline identity is critical for
357 ensuring a normal blastema morphology. We suggest that in lateral amputations that require formation of a
358 new midline, a similar system of pre-existing dorsoventral information, possibly via repulsive ventral
359 signals, is likely used for forming a new dorsal midline important for outgrowth.

360 Whole body regeneration in planarians depends on axis information systems encoded in muscle
361 cells. Our study finds muscle-expressed ligands signaling through muscle-expressed receptors to control
362 regionalization of muscle identity. These observations suggest that regional communication could take

place directly between muscle cells. Alternatively, given that *dcc-2* and other netrin receptors are expressed more broadly, an alternative possible mechanism for pattern formation could involve the use of positional cues from muscle to influence regionalization through control of stem cell differentiation into distinct muscle domains. Netrins have dorsoventral expression domains opposing BMP in multiple organisms, including in planarians, hemichordates (Lowe et al., 2006), acoels (Srivastava et al., 2014), Drosophila (Harris et al., 1996; Mitchell et al., 1996), and within the vertebrate neural tube (Serafini et al., 1994; Lai Wing Sun et al., 2011). In addition, Netrins have expression in body wall muscle in planarians (Witchley et al., 2013), acoels (Raz et al., 2017), Drosophila, and *C. elegans* (Ishii et al., 1992). Our observations point to an ancient use of Netrins for linking dorsoventral and midline identity through muscle. The involvement of multiple Netrins and receptors for controlling dorsal midline muscle and blastema morphology suggests the possibility of a dorsoventral code of these factors that guide patterning of the blastema in order to restore bilateral symmetry during regeneration.

Acknowledgements

We thank members of the Petersen lab for critical comments. CP acknowledges funding from NIGMS R01GM129339, R01GM130835, and pilot project funding from the NSF-Simons Center for Quantitative Biology at Northwestern University, an NSF (1764421)-Simons/SFARI (597491-RWC) MathBioSys Research Center.

Author contributions: CP conceived of the study and acquired funding, ES designed and conducted experiments, CP and ES wrote the manuscript.

Declaration of Interests: There are no competing interests.

389 **Figure Legends**

390 **Figure 1. *pitx* controls differentiation of *bambi-2*+ dorsal midline longitudinal muscle cells.**

391 **(A)** Analysis of prior scRNAseq data (Fincher et al 2018) comparing transcriptomes of dorsal muscle
392 midline cells co-expressing *bambi-2(dd23400)* and *slit* versus *collagen+* muscle lacking *bambi-2* and *slit*
393 expression. Table shows log2-fold change (upper bound, ub) from scde analysis. Right panels show WISH
394 of candidates with expression on the posterior midline. Images represent 3-4 animals per condition. **(B)**
395 Animals were fixed and FISH was performed to detect *islet* or *pitx* expression on the dorsal midline in the
396 anterior (left) or posterior (right). Arrows indicate expression on the dorsal midline. **(C)** Homeostatic RNAi
397 (8 feedings dsRNA) to inhibit transcription factors specific for midline cells (*islet, pitx*), L-muscle (*myoD*),
398 and C-muscle (*nkx1-1*) followed by FISH to detect *bambi-2*. **(D)** FISH other midline markers after *pitx*,
399 *islet* or *bambi-2* RNAi**.** Bars, 100 (B) or 200 microns (A,C).

400

401 **Figure 2. *bambi-2*+ dorsal midline longitudinal muscle cells are required for blastema outgrowth in**
402 **fragments lacking a midline.**

403 **(A)** Live images showing *islet* and *pitx* are required for posterior regeneration (arrows). **(B)** Live images
404 showing *islet* and *pitx* are required for blastema formation in regenerating fragments lacking midline.
405 Yellow brackets indicate blastema width, arrows indicate failed blastema formation. Right,
406 quantifications of blastema width divided by animal width. ***, $p<0.001$ by two-tailed unpaired t-tests
407 compared to control RNAi conditions. **(C)** In lateral regenerating fragments that initially lack midline
408 tissue, *islet(RNAi)* reduced and *pitx(RNAi)* nearly eliminated the ability to regenerate a *slit*-expressing
409 midline, while expression of lateral epidermal marker *laminB* occurred normally (arrows). Bars, 200
410 microns. Numbers in panels indicate fraction of animals as shown.

411

412

413

414 **Figure 3. Lateral regeneration progressively restores midline identity through injury-induced**
415 **expression and growth.**
416 FISH of *bambi-2* expression during a timeseries of the regeneration of asymmetric lateral fragments that
417 must regenerate the dorsal midline. Bottom, quantifications of the relative and absolute locations of the
418 *bambi-2+* cells with respect to the wound edge (left), the relative size of the *bambi-2+* domain and size of
419 pre-existing tissue domain lateral to the *bambi-2* domain (center), and absolute width of the regenerating
420 fragments. *bambi-2* expression first arises at the lateral wound edge by 24 hours, followed by a
421 progressive relative movement toward the left/right center of the fragment, rather than a mechanism that
422 directly places these cells centrally. n=12-15 animals. * $p<0.05$, ** $p<0.01$, *** $p<0.001$ by two-tailed
423 unpaired t-tests.
424
425 **Figure 4. Netrins and Netrin receptors are expressed in dorsoventral domains in muscle cells.**
426 **(A)** FISH images showing *netrins* are expressed in along either ventromedial (*netrin-2, netrin-4, netrin-5)*
427 or lateral (*netrin-1, netrin-3)* domains. Each image shows a ventral view. N=5-6 animals. **(B)** FISH images
428 showing Netrin receptors are expressed in along either dorsomedial (*unc5-C, unc5-E, dcc-2)* or lateral
429 (*unc5-A, unc5-B, unc5-D, dcc-1)* domains (4-7 animals probed per condition). (C) Images of cross-sections,
430 dorsal side top. FISH images showing *netrins* are expressed in along either ventromedial (*netrin-2, netrin-*
431 *4, netrin-5)* or lateral (*netrin-1, netrin-3)* domains (4-6 animals probed per condition) FISH images showing
432 Netrin receptors are expressed in along either dorsomedial (*unc5-C, unc5-E, dcc-2)* or lateral (*unc5-A, unc5-*
433 *B, unc5-D, dcc-1)* domains. Bars, 100 (A,B) or 50 microns (C). Arrows indicate expression of each tested
434 gene coincident with *collagen+* muscle. (D) Cartoon of planarian cross-section displaying the approximate
435 expression domains for each Netrin and Netrin receptor.
436
437 **Figure 5. Netrins act cooperatively to control blastema morphology and regeneration.**
438 **(A)** Live images showing RNAi of individual *netrins* results in normal regeneration. (10 animals per
439 condition). **(B)** Simultaneous inhibition of all five Netrins causes regeneration of blastemas with an

440 indentation in the posterior and pointed morphology in the anterior, as well as weakly penetrant
441 regeneration failure in head and tail fragments (arrows). **(C)** RNAi of *unc5-C, unc5-E* and *dcc-2*
442 individually or in combination results in indented blastemas (arrows). Bars, 200 microns.
443
444 **Figure 6. Netrins control midline muscle cell organization and organization of muscle around the**
445 **midline (A)** FISH showing expression of patterning factors following inhibition of each Netrin. Midline
446 (*bambi-2, slit*) and anterior pole cells (*notum)* are expanded, while lateral (*wnt5*), posterior (*wnt1*), and
447 dorsoventral markers (*bmp-4, admp-1*) appear normal. *admp-* and *notum*-stained animals are from
448 regenerating tail fragments, all other panels show regenerating trunk fragments. Insets show enlargements
449 of *bambi-2* and *slit* expression **(B)** FISH showing expanded *bambi-2* expression domain following *unc5-*
450 *C,-E,dcc-2* RNAi. Insets show enlargements of *bambi-2* expression. **(C)** Quantification of midline
451 expansion normalized to body width in each condition. Bars show standard error of 5-10 replicates, *** p
452 <0.001 by 2-tailed unpaired t-test. **(D)** Immunostaining with 6G10 antibody to visualize muscle fiber
453 morphology after *netrin-1;-2;-3;-4;-5* RNAi and *unc5-C;unc5-E;dcc-2* RNAi in anterior (top) or posterior
454 (bottom) blastemas. Muscle morphology was disrupted at locations of the indented blastema. Animals were
455 fixed after 8 dsRNA feedings and 14 days of regeneration in all panels. Bars, 200 (A-B) or 100 microns
456 (D).
457
458 **Figure 7. Model**
459 **(A)** In regeneration of lateral fragments, the *bambi-2*+ dorsal midline muscle is re-established near the
460 wound site and not the geometric center of the fragment. *pitx* and *islet* are necessary both for *bambi-2*
461 expression and blastema outgrowth that restores bilateral symmetry (B) Three ventral netrins likely act
462 through dorsal netrin receptors to restrict the location of the *bambi-2*+ cells.
463
464
465

466

467 **Supplemental Figures**

468 **Figure S1. dd23400/*bambi-2* encodes a BAMBI decoy receptor**

469 **(A)** Sequence alignment of dd23400 with BAMBI factors with conserved residues highlighted in red. Green bar
470 indicates location of ActR domain. dd23400 has a weakly detected ActR domain (aa4-84, evalue 0.14), possesses
471 a transmembrane domain (aa158-180, TMHMMv2.0) and like other BAMBI homologs lacks an intracellular
472 kinase activation domain. DELTA Blast of dd23400 followed by PSI-blast (3 rounds, 500 iterations) recovers
473 BAMBI orthologs from several species, including BAMBI from Osmia bicornis (evalue=1e-22), Megachile
474 rotundata (evalue=3e-22) and Apis mellifera (evalue=3e-20).**(B)** Bayesian inference phylogenetic tree generated
475 from alignment with MUSCLE and calculated with MrBayes v3.2.3 using a GTR substitution model with
476 gamma-distributed rate variation across sites and a proportion of invariable sites. Runs of 50000 generations
477 converged with an average standard deviation of split frequencies <0.01 and 25% of trees were discarded as
478 burn-in. Tree displayed using FigTree v1.4.4 with branch labels indicating posterior probabilities. BAMBI
479 sequences from Owenia fusiformis (Of, CAC9588793.1), Octopus bimaculoides (Ob, XP_014790456.1),
480 Argiope bruennichi (Ab, KAF8794778.1), Araneus ventricosus (Av, GBL98371.1), Stegodyphus mimosarum
481 (Sm, KFM81221.1), Xenopus laevis (Xl, CAB56858.1), Mus musculus (Mm, NP_036474.1), and
482 Branchiostoma floridae (Bf, XP_035688850.1).Tree is rooted using BMPR1 receptors from Brachiostoma
483 floridae (Bf), Danio rerio (Dr), and Mus musculus (Mm).

484

485 **Figure S2. Expression of netrins and netrin receptors from cell atlas.**

486 Plots of Netrin and Netrin receptor gene expression from a planarian cell atlas (Fincher et al., 2018 ;
487 digiworm.wi.mit.edu). Top cartoon shows cluster identities. Netrins and receptors have expression in
488 muscle cells and also in other cell types.

489

490 **Figure S3. qPCR validating knockdown.**

491 dsRNAs targeting netrins -1, -2, -3, -4, and -5 were mixed together and delivered to animals by feeding 6
492 times over 2 weeks ("pan-net") and compared to animals treated with control dsRNA. RNA was harvested
493 and qPCR conducted to measure knockdown of each Netrin factor as indicated, using *clathrin* transcript as
494 a normalizing control. Bars show standard error of 4 replicates, ***P<0.001 by 2-tailed unpaired t-test.
495
496 **Figure S4. Netrins -1, -2, -4, and -5 promote proper anterior blastema morphology while *net-2, -4,***
497 **and -5 promote posterior blastema morphology.**
498 (A) Graph showing regeneration score of anterior blastemas for all combinations of Netrin RNAi. n=7-10
499 animals. Animals were qualitatively scored based on the degree of pointedness from P0 (normal), P1
500 (subtle), P2 (pointy), to P3 (highly pointed). In order to compare different conditions with varying
501 penetrance and expressivity, a weighted average phenotype strength score was computed for each treatment
502 by summing the numbers of animals scored in each category multiplied by a scalar of increasing size for
503 higher expressivity (i.e., score = [(# animals in P1) + 2 x (# animals in P2) +3 x (# animals in P3)]/(total
504 number scored)). Average phenotype strength scores were normalized to the value from inhibition of all
505 five Netrins for comparison. Right- Representative images of degrees of blastema pointedness in different
506 combinations of Netrin inhibitions. (B) Graph showing percentage of indented posterior blastemas for all
507 combinations of Netrin RNAi. n=7-10 animals. Right- Representative images of degrees of indented-ness
508 in different combinations of Netrin inhibitions. (C) Live images showing *netrin-1;-2;-3;-4;-5* are not
509 required for blastema formation in regenerating fragments lacking midline.
510
511 **Figure S5. *netrins* are not required for wound-induced expression of *notum* and *follistatin.***
512 **(A)** Animals were fixed following 8 dsRNA feedings and fixed either 6 or 24 hours after injury. FISH
513 showing *notum* or *fst* expression is unchanged in All Netrin RNAi. n=>10 animals. In panel A bars are 200
514 microns.
515
516

517

518

519 **Materials and Methods**

520 **Experimental Model**

521 Asexual *Schmidtea mediterranea* animals (CIW4 strain) were maintained in 1x Montjuic salts
522 between 18–20°C. Animals were fed a puree of beef liver and starved for at least 7 days before experiments.

523

524 **In situ hybridizations**

525 Animals were fixed and bleached as described previously (Pearson et al., 2009; King and Newmark, 2013).
526 Riboprobes (digoxigenin- or fluorescein-labeled) were synthesized by in vitro transcription (Pearson et al.,
527 2009; King and Newmark, 2013). Antibodies were used in TNTx/10% horse serum
528 (Roche, Basel Switzerland) at a concentration of 1:2000 for anti-DIG-POD (Roche, Basel Switzerland),
529 and 1:2000 for anti-FL- (Roche), or 1:4000 for anti-dig-alkaline phosphatase used in colorimetric in situ
530 hybridizations (Roche, Basel Switzerland). For multiplex FISH, peroxidase conjugated enzyme activity
531 was quenched between tyramide reactions by sodium azide treatment (100 mM in 1xTNTx) for 45 min at
532 room temperature. Nuclear counterstaining was performed using Hoechst 33342 (Invitrogen, 1:1000 in
533 1xPBSTx for 45 minutes). Colorimetric in situ hybridizations were developed using NBT/BCIP as
534 described previously (Lander and Petersen, 2016). Primer sequences used for cloning to generate riboprobes
535 are listed in Table S2.

536

537 **Immunostaining**

538 Animals were fixed the same as in FISH (King and Newmark, 2013). Bleaching was performed in
539 80% methanol, 20% hydrogen peroxide on a lightbox overnight. Following rehydration washes, animals
540 were washed and rocked in PBSTx/10% horse serum (Roche, Basel Switzerland) 8 times for 6 hours.
541 Animals were incubated in the anti-muscle mouse monoclonal antibody 6G10-2C7 (Iowa Hybridoma Bank)
542 at 1:1000 overnight, then washed in PBSTx/10% horse serum 8 times for 6 hours. Animals were incubated

543 overnight in an anti-mouse Dig conjugated antibody in PBSTx/10% horse serum. After 8 PBSTx washes,
544 tyramide amplification was performed using commercial tyramide kit. Finally, animals were washed in
545 PBSTx 8 times, 20 minutes each.
546
547 **RNAi administration**
548 RNAi by feeding was performed in vitro transcribed dsRNA mixed with liver paste and 5% red
549 food dye (Rouhana et al., 2013). For single RNAi experiments, dsRNA at a concentration of 2-4 ug/ul was
550 mixed with liver in a 1:5 ratio. In RNAi experiments with multiple dsRNAs, each dsRNA was mixed with
551 liver for a total concentration of 1:10 for each dsRNA. In all RNAi experiments animals were fed RNAi
552 food every 2-4 days for the length of experiment indicated. For homeostatic experiments, animals were
553 starved for at least 5 days before fixing. In regeneration experiments, animals were amputated the same day
554 of the last feeding, or in Figure 1C, 1D, Figure S4 at 5 days after the final RNAi feeding. dsRNA targeting
555 the *Photinus pyralis* luciferase (not present in the planarian genome) was used as a negative control RNAi
556 condition. Primers sequences used for RNAi are listed in Table S2.
557
558 **Image Acquisition and Quantification**
559 Live images of animals were performed with a Leica M210F dissecting scope with a Leica DFC295 camera.
560 FISH images were performed a Leica DM5500B compound microscope with optical sectioning by Optigrid
561 structured illumination or a Leica Stellaris or Leica TCS SPE confocal compound microscopes. Fluorescent
562 images collected by compound microscopy are maximum projections of a z-stack and adjusted for
563 brightness and contrast using Metamorph, Adobe Photoshop, ImageJ, or Leica LAS.
564
565 **qPCR**
566 RNA was harvested from 4 biological replicates of 4 animals per condition using a Turrex tissue
567 homogenizer. cDNAs were synthesized using oligo-dT and Superscript III reverse transcriptase (Life
568 Technologies) for 1 hour at 50°C. EvaGreen qPCR mastermix (Midwest Scientific BEQPCR-S) was used

569 for amplification and detection. Per-sample log2-fold change expression were determined by the delta-
570 delta Ct method, normalizing to expression of housekeeping gene clathrin probe set control and to RNAi
571 negative controls targeting *Photinus pyralis* luciferase (not present in planarian genome). Statistical
572 significance was determined through unpaired two-tailed t-tests comparing ddCt values between control
573 RNAi and target RNAi conditions. Primers for qPCR: *netrin-1* (5'-taaagagcatcagggtctatgtga -3', 5'-
574 ataatatcgacgcttcaatttcca-3'); *netrin-2* (5'-gaattggtatgacaagacaactgc-3', 5'-gttttgcgtcgcatatactacaat-3');
575 *netrin-3* (5'-cgaaaccctatgtaaaaagaagga-3', 5'-cccttggagattttataggacaga-3') ; *netrin-4* (5'-
576 cctgttaaattgaaatcgctctct-3', 5'-aataaaataatttggggatgctga-3') ; *netrin-5* (5'-tgcacaaaatgctacatttgaagt-3', 5'-
577 atcctttctgaccgcatgtact-3'); *clathrin* (5'-agccgcatgtagttggttagtg-3', 5'-agtctacagaaaaccatcaattgtttcaaa-3').
578
579 **scRNAseq differential gene expression testing**
580 We mined a prior single-cell RNAseq atlas generated by DropSeq (Fincher et al., 2018) and recovered 15
581 *dd23400+slit+* cells (at least 1 read for *bambi-2/dd23400* and at least 2 reads for *slit*) and compared these
582 to 143 randomly selected muscle cells (at least 7 reads for muscle marker *collagen* dd840 and no reads for
583 *dd23400* or *slit*) and analyzed for differential gene expression using the Single Cell Differential Gene
584 Expression (scde) method (Kharchenko et al., 2014). Table S1 shows results of differential testing along
585 with identity of cells selected for analysis.
586
587 **Phylogenetic analysis**
588 Bayesian inference phylogenetic tree was generated from alignment with MUSCLE and calculated with
589 MrBayes v3.2.3 using a GTR substitution model with gamma-distributed rate variation across sites and a
590 proportion of invariable sites. Runs of 50000 generations converged with an average standard deviation of
591 split frequencies <0.01 and 25% of trees were discarded as burn-in.
592
593
594

References

ALMUEDO-CASTILLO, M., SALÓ, E. & ADELL, T. 2011. Dishevelled is essential for neural connectivity and planar cell polarity in planarians. *Proceedings of the National Academy of Sciences,* 108**,** 2813-2818.

BONAR, N. A., GITTIN, D. I. & PETERSEN, C. P. 2022. Src acts with WNT/FGFRL signaling to pattern the planarian anteroposterior axis. *Development,* 149.

BOYER, N. P. & GUPTON, S. L. 2018. Revisiting Netrin-1: One Who Guides (Axons). *Front Cell Neurosci,* 12**,** 221.

CEBRIA, F. 2016. Planarian Body-Wall Muscle: Regeneration and Function beyond a Simple Skeletal Support. *Front Cell Dev Biol,* 4**,** 8.

CEBRIA, F., GUO, T., JOPEK, J. & NEWMARK, P. A. 2007. Regeneration and maintenance of the planarian midline is regulated by a slit orthologue. *Dev Biol,* 307**,** 394-406.

CEBRIA, F., KOBAYASHI, C., UMESONO, Y., NAKAZAWA, M., MINETA, K., IKEO, K., GOJOBORI, T., ITOH, M., TAIRA, M., SANCHEZ ALVARADO, A. & AGATA, K. 2002. FGFR-related gene nou-darake restricts brain tissues to the head region of planarians. *Nature,* 419**,** 620-4.

CEBRIA, F. & NEWMARK, P. A. 2005. Planarian homologs of netrin and netrin receptor are required for proper regeneration of the central nervous system and the maintenance of nervous system architecture. *Development,* 132**,** 3691-703.

CHAN, S. S., ZHENG, H., SU, M. W., WILK, R., KILLEEN, M. T., HEDGECOCK, E. M. & CULOTTI, J. G. 1996. UNC-40, a C. elegans homolog of DCC (Deleted in Colorectal Cancer), is required in motile cells responding to UNC-6 netrin cues. *Cell,* 87**,** 187-95.

CLOUTIER, J. K., MCMANN, C. L., ODERBERG, I. M. & REDDIEN, P. W. 2021. activin-2 is required for regeneration of polarity on the planarian anterior-posterior axis. *PLoS Genet,* 17**,** e1009466.

COLAVITA, A. & CULOTTI, J. G. 1998. Suppressors of ectopic UNC-5 growth cone steering identify eight genes involved in axon guidance in Caenorhabditis elegans. *Dev Biol,* 194**,** 72-85.

CURRIE, K. W. & PEARSON, B. J. 2013. Transcription factors lhx1/5-1 and pitx are required for the maintenance and regeneration of serotonergic neurons in planarians. *Development,* 140**,** 3577-88.

DALVIN, S., ANSELMO, M. A., PRODHAN, P., KOMATSUZAKI, K., SCHNITZER, J. J. & KINANE, T. B. 2003. Expression of Netrin-1 and its two receptors DCC and UNC5H2 in the developing mouse lung. *Gene Expr Patterns,* 3**,** 279-83.

DE BREUCK, S., LARDON, J., ROOMAN, I. & BOUWENS, L. 2003. Netrin-1 expression in fetal and regenerating rat pancreas and its effect on the migration of human pancreatic duct and porcine islet precursor cells. *Diabetologia,* 46**,** 926-33.

FAZELI, A., DICKINSON, S. L., HERMISTON, M. L., TIGHE, R. V., STEEN, R. G., SMALL, C. G., STOECKLI, E. T., KEINO-MASU, K., MASU, M., RAYBURN, H., SIMONS, J., BRONSON, R. T., GORDON, J. I., TESSIER-LAVIGNE, M. & WEINBERG, R. A. 1997. Phenotype of mice lacking functional Deleted in colorectal cancer (Dcc) gene. *Nature,* 386**,** 796-804.

639 FINCHER, C. T., WURTZEL, O., DE HOOG, T., KRAVARIK, K. M. & REDDIEN, P. W.
640 2018. Cell type transcriptome atlas for the planarian Schmidtea mediterranea. *Science,*
641 360.
642 FINCI, L. I., KRUGER, N., SUN, X., ZHANG, J., CHEGKAZI, M., WU, Y., SCHENK, G.,
643 MERTENS, H. D. T., SVERGUN, D. I., ZHANG, Y., WANG, J. H. & MEIJERS, R.
644 2014. The crystal structure of netrin-1 in complex with DCC reveals the bifunctionality
645 of netrin-1 as a guidance cue. *Neuron,* 83**,** 839-849.
646 GAVINO, M. A. & REDDIEN, P. W. 2011. A Bmp/Admp regulatory circuit controls
647 maintenance and regeneration of dorsal-ventral polarity in planarians. *Curr Biol,* 21**,** 294-
648 9.
649 GAVINO, M. A., WENEMOSER, D., WANG, I. E. & REDDIEN, P. W. 2013. Tissue absence
650 initiates regeneration through follistatin-mediated inhibition of activin signaling. *Elife,* 2**,**
651 e00247.
652 GLISE, B., MILLER, C. A., CROZATIER, M., HALBISEN, M. A., WISE, S., OLSON, D. J.,
653 VINCENT, A. & BLAIR, S. S. 2005. Shifted, the Drosophila ortholog of Wnt inhibitory
654 factor-1, controls the distribution and movement of Hedgehog. *Dev Cell,* 8**,** 255-66.
655 GURLEY, K. A., ELLIOTT, S. A., SIMAKOV, O., SCHMIDT, H. A., HOLSTEIN, T. W. &
656 SANCHEZ ALVARADO, A. 2010. Expression of secreted Wnt pathway components
657 reveals unexpected complexity of the planarian amputation response. *Dev Biol,* 347**,** 24-
658 39.
659 GURLEY, K. A., RINK, J. C. & SANCHEZ ALVARADO, A. 2008. Beta-catenin defines head
660 versus tail identity during planarian regeneration and homeostasis. *Science,* 319**,** 323-7.
661 HAMELIN, M., ZHOU, Y., SU, M. W., SCOTT, I. M. & CULOTTI, J. G. 1993. Expression of
662 the UNC-5 guidance receptor in the touch neurons of C. elegans steers their axons
663 dorsally. *Nature,* 364**,** 327-30.
664 HARRIS, R., SABATELLI, L. M. & SEEGER, M. A. 1996. Guidance cues at the Drosophila
665 CNS midline: identification and characterization of two Drosophila Netrin/UNC-6
666 homologs. *Neuron,* 17**,** 217-28.
667 HAYASHI, T., MOTOISHI, M., YAZAWA, S., ITOMI, K., TANEGASHIMA, C.,
668 NISHIMURA, O., AGATA, K. & TARUI, H. 2011. A LIM-homeobox gene is required
669 for differentiation of Wnt-expressing cells at the posterior end of the planarian body.
670 *Development,* 138**,** 3679-88.
671 HEDGECOCK, E. M., CULOTTI, J. G. & HALL, D. H. 1990. The unc-5, unc-6, and unc-40
672 genes guide circumferential migrations of pioneer axons and mesodermal cells on the
673 epidermis in C. elegans. *Neuron,* 4**,** 61-85.
674 HONG, K., HINCK, L., NISHIYAMA, M., POO, M. M., TESSIER-LAVIGNE, M. & STEIN,
675 E. 1999. A ligand-gated association between cytoplasmic domains of UNC5 and DCC
676 family receptors converts netrin-induced growth cone attraction to repulsion. *Cell,* 97**,**
677 927-41.
678 HSIEH, J. C., KODJABACHIAN, L., REBBERT, M. L., RATTNER, A., SMALLWOOD, P.
679 M., SAMOS, C. H., NUSSE, R., DAWID, I. B. & NATHANS, J. 1999. A new secreted
680 protein that binds to Wnt proteins and inhibits their activities. *Nature,* 398**,** 431-6.
681 IGLESIAS, M., GOMEZ-SKARMETA, J. L., SALO, E. & ADELL, T. 2008. Silencing of
682 Smed-betacatenin1 generates radial-like hypercephalized planarians. *Development,* 135**,**
683 1215-21.

ISHII, N., WADSWORTH, W. G., STERN, B. D., CULOTTI, J. G. & HEDGECOCK, E. M. 1992. UNC-6, a laminin-related protein, guides cell and pioneer axon migrations in C. elegans. *Neuron,* 9**,** 873-81.

KANG, J. S., YI, M. J., ZHANG, W., FEINLEIB, J. L., COLE, F. & KRAUSS, R. S. 2004. Netrins and neogenin promote myotube formation. *J Cell Biol,* 167**,** 493-504.

KEINO-MASU, K., MASU, M., HINCK, L., LEONARDO, E. D., CHAN, S. S., CULOTTI, J. G. & TESSIER-LAVIGNE, M. 1996. Deleted in Colorectal Cancer (DCC) encodes a netrin receptor. *Cell,* 87**,** 175-85.

KELEMAN, K. & DICKSON, B. J. 2001. Short- and long-range repulsion by the Drosophila Unc5 netrin receptor. *Neuron,* 32**,** 605-17.

KENNEDY, T. E., SERAFINI, T., DE LA TORRE, J. R. & TESSIER-LAVIGNE, M. 1994. Netrins are diffusible chemotropic factors for commissural axons in the embryonic spinal cord. *Cell,* 78**,** 425-35.

KHARCHENKO, P. V., SILBERSTEIN, L. & SCADDEN, D. T. 2014. Bayesian approach to single-cell differential expression analysis. *Nat Methods,* 11**,** 740-2.

KING, R. S. & NEWMARK, P. A. 2013. In situ hybridization protocol for enhanced detection of gene expression in the planarian Schmidtea mediterranea. *BMC Dev Biol,* 13**,** 8.

KOLODZIEJ, P. A., TIMPE, L. C., MITCHELL, K. J., FRIED, S. R., GOODMAN, C. S., JAN, L. Y. & JAN, Y. N. 1996. frazzled encodes a Drosophila member of the DCC immunoglobulin subfamily and is required for CNS and motor axon guidance. *Cell,* 87**,** 197-204.

LAI WING SUN, K., CORREIA, J. P. & KENNEDY, T. E. 2011. Netrins: versatile extracellular cues with diverse functions. *Development,* 138**,** 2153-69.

LANDER, R. & PETERSEN, C. P. 2016. Wnt, Ptk7, and FGFRL expression gradients control trunk positional identity in planarian regeneration. *Elife,* 5.

LI, D. J., MCMANN, C. L. & REDDIEN, P. W. 2019. Nuclear receptor NR4A is required for patterning at the ends of the planarian anterior-posterior axis. *Elife,* 8.

LIU, Y., STEIN, E., OLIVER, T., LI, Y., BRUNKEN, W. J., KOCH, M., TESSIER-LAVIGNE, M. & HOGAN, B. L. 2004. Novel role for Netrins in regulating epithelial behavior during lung branching morphogenesis. *Curr Biol,* 14**,** 897-905.

LLAMBI, F., CAUSERET, F., BLOCH-GALLEGO, E. & MEHLEN, P. 2001. Netrin-1 acts as a survival factor via its receptors UNC5H and DCC. *EMBO J,* 20**,** 2715-22.

LOWE, C. J., TERASAKI, M., WU, M., FREEMAN, R. M., JR., RUNFT, L., KWAN, K., HAIGO, S., ARONOWICZ, J., LANDER, E., GRUBER, C., SMITH, M., KIRSCHNER, M. & GERHART, J. 2006. Dorsoventral patterning in hemichordates: insights into early chordate evolution. *PLoS Biol,* 4**,** e291.

MARZ, M., SEEBECK, F. & BARTSCHERER, K. 2013. A Pitx transcription factor controls the establishment and maintenance of the serotonergic lineage in planarians. *Development,* 140**,** 4499-509.

MÄRZ, M., SEEBECK, F. & BARTSCHERER, K. 2013. A Pitx transcription factor controls the establishment and maintenance of the serotonergic lineage in planarians. *Development,* 140**,** 4499-4509.

MEHLEN, P., RABIZADEH, S., SNIPAS, S. J., ASSA-MUNT, N., SALVESEN, G. S. & BREDESEN, D. E. 1998. The DCC gene product induces apoptosis by a mechanism requiring receptor proteolysis. *Nature,* 395**,** 801-4.

MITCHELL, K. J., DOYLE, J. L., SERAFINI, T., KENNEDY, T. E., TESSIER-LAVIGNE, M., GOODMAN, C. S. & DICKSON, B. J. 1996. Genetic analysis of Netrin genes in Drosophila: Netrins guide CNS commissural axons and peripheral motor axons. *Neuron,* 17**,** 203-15.

MOLINA, M. D., SALO, E. & CEBRIA, F. 2007. The BMP pathway is essential for re-specification and maintenance of the dorsoventral axis in regenerating and intact planarians. *Dev Biol,* 311**,** 79-94.

ODERBERG, I. M., LI, D. J., SCIMONE, M. L., GAVINO, M. A. & REDDIEN, P. W. 2017. Landmarks in Existing Tissue at Wounds Are Utilized to Generate Pattern in Regenerating Tissue. *Curr Biol,* 27**,** 733-742.

ONICHTCHOUK, D., CHEN, Y. G., DOSCH, R., GAWANTKA, V., DELIUS, H., MASSAGUE, J. & NIEHRS, C. 1999. Silencing of TGF-beta signalling by the pseudoreceptor BAMBI. *Nature,* 401**,** 480-5.

ORII, H. & WATANABE, K. 2007. Bone morphogenetic protein is required for dorso-ventral patterning in the planarian Dugesia japonica. *Dev Growth Differ,* 49**,** 345-9.

OWEN, J. H., WAGNER, D. E., CHEN, C. C., PETERSEN, C. P. & REDDIEN, P. W. 2015. teashirt is required for head-versus-tail regeneration polarity in planarians. *Development,* 142**,** 1062-72.

PEARSON, B. J., EISENHOFFER, G. T., GURLEY, K. A., RINK, J. C., MILLER, D. E. & SANCHEZ ALVARADO, A. 2009. Formaldehyde-based whole-mount in situ hybridization method for planarians. *Dev Dyn,* 238**,** 443-50.

PETERSEN, C. P. & REDDIEN, P. W. 2008. Smed-betacatenin-1 is required for anteroposterior blastema polarity in planarian regeneration. *Science,* 319**,** 327-30.

PETERSEN, C. P. & REDDIEN, P. W. 2009. A wound-induced Wnt expression program controls planarian regeneration polarity. *Proc Natl Acad Sci U S A,* 106**,** 17061-6.

PETERSEN, C. P. & REDDIEN, P. W. 2011. Polarized notum activation at wounds inhibits Wnt function to promote planarian head regeneration. *Science,* 332**,** 852-5.

RAZ, A. A., SRIVASTAVA, M., SALVAMOSER, R. & REDDIEN, P. W. 2017. Acoel regeneration mechanisms indicate an ancient role for muscle in regenerative patterning. *Nat Commun,* 8**,** 1260.

REDDIEN, P. W. 2018. The Cellular and Molecular Basis for Planarian Regeneration. *Cell,* 175**,** 327-345.

REDDIEN, P. W., BERMANGE, A. L., KICZA, A. M. & SANCHEZ ALVARADO, A. 2007. BMP signaling regulates the dorsal planarian midline and is needed for asymmetric regeneration. *Development,* 134**,** 4043-51.

REUTER, H., MARZ, M., VOGG, M. C., ECCLES, D., GRIFOL-BOLDU, L., WEHNER, D., OWLARN, S., ADELL, T., WEIDINGER, G. & BARTSCHERER, K. 2015. Beta-catenin-dependent control of positional information along the AP body axis in planarians involves a teashirt family member. *Cell Rep,* 10**,** 253-65.

ROBERTS-GALBRAITH, R. H. & NEWMARK, P. A. 2013. Follistatin antagonizes activin signaling and acts with notum to direct planarian head regeneration. *Proc Natl Acad Sci U S A,* 110**,** 1363-8.

ROSS, K. G., OMURO, K. C., TAYLOR, M. R., MUNDAY, R. K., HUBERT, A., KING, R. S. & ZAYAS, R. M. 2015. Novel monoclonal antibodies to study tissue regeneration in planarians. *BMC Dev Biol,* 15**,** 2.

774 ROUHANA, L., WEISS, J. A., FORSTHOEFEL, D. J., LEE, H., KING, R. S., INOUE, T.,
775 SHIBATA, N., AGATA, K. & NEWMARK, P. A. 2013. RNA interference by feeding in
776 vitro-synthesized double-stranded RNA to planarians: methodology and dynamics. *Dev*
777 *Dyn,* 242**,** 718-30.
778 SCHAD, E. G. & PETERSEN, C. P. 2020. STRIPAK Limits Stem Cell Differentiation of a
779 WNT Signaling Center to Control Planarian Axis Scaling. *Curr Biol,* 30**,** 254-263 e2.
780 SCIMONE, M. L., ATABAY, K. D., FINCHER, C. T., BONNEAU, A. R., LI, D. J. &
781 REDDIEN, P. W. 2020. Muscle and neuronal guidepost-like cells facilitate planarian
782 visual system regeneration. *Science,* 368.
783 SCIMONE, M. L., COTE, L. E. & REDDIEN, P. W. 2017. Orthogonal muscle fibres have
784 different instructive roles in planarian regeneration. *Nature,* 551**,** 623-628.
785 SCIMONE, M. L., COTE, L. E., ROGERS, T. & REDDIEN, P. W. 2016. Two FGFRL-Wnt
786 circuits organize the planarian anteroposterior axis. *Elife,* 5.
787 SCIMONE, M. L., WURTZEL, O., MALECEK, K., FINCHER, C. T., ODERBERG, I. M.,
788 KRAVARIK, K. M. & REDDIEN, P. W. 2018. foxF-1 Controls Specification of Non-
789 body Wall Muscle and Phagocytic Cells in Planarians. *Curr Biol,* 28**,** 3787-3801 e6.
790 SERAFINI, T., KENNEDY, T. E., GALKO, M. J., MIRZAYAN, C., JESSELL, T. M. &
791 TESSIER-LAVIGNE, M. 1994. The netrins define a family of axon outgrowth-
792 promoting proteins homologous to C. elegans UNC-6. *Cell,* 78**,** 409-24.
793 SRINIVASAN, K., STRICKLAND, P., VALDES, A., SHIN, G. C. & HINCK, L. 2003. Netrin-
794 1/neogenin interaction stabilizes multipotent progenitor cap cells during mammary gland
795 morphogenesis. *Dev Cell,* 4**,** 371-82.
796 SRIVASTAVA, M. 2022. Studying development, regeneration, stem cells, and more in the acoel
797 Hofstenia miamia. *Curr Top Dev Biol,* 147**,** 153-172.
798 SRIVASTAVA, M., MAZZA-CURLL, K. L., VAN WOLFSWINKEL, J. C. & REDDIEN, P.
799 W. 2014. Whole-body acoel regeneration is controlled by Wnt and Bmp-Admp signaling.
800 *Curr Biol,* 24**,** 1107-13.
801 STUCKEMANN, T., CLELAND, J. P., WERNER, S., THI-KIM VU, H., BAYERSDORF, R.,
802 LIU, S. Y., FRIEDRICH, B., JULICHER, F. & RINK, J. C. 2017. Antagonistic Self-
803 Organizing Patterning Systems Control Maintenance and Regeneration of the
804 Anteroposterior Axis in Planarians. *Dev Cell,* 40**,** 248-263 e4.
805 TEWARI, A. G., STERN, S. R., ODERBERG, I. M. & REDDIEN, P. W. 2018. Cellular and
806 Molecular Responses Unique to Major Injury Are Dispensable for Planarian
807 Regeneration. *Cell Rep,* 25**,** 2577-2590 e3.
808 VOGG, M. C., GALLIOT, B. & TSIAIRIS, C. D. 2019. Model systems for regeneration: Hydra.
809 *Development,* 146.
810 VU, H. T., MANSOUR, S., KUCKEN, M., BLASSE, C., BASQUIN, C., AZIMZADEH, J.,
811 MYERS, E. W., BRUSCH, L. & RINK, J. C. 2019. Dynamic Polarization of the
812 Multiciliated Planarian Epidermis between Body Plan Landmarks. *Dev Cell,* 51**,** 526-542
813 e6.
814 WAGNER, D. E., WANG, I. E. & REDDIEN, P. W. 2011. Clonogenic neoblasts are pluripotent
815 adult stem cells that underlie planarian regeneration. *Science,* 332**,** 811-6.
816 WITCHLEY, J. N., MAYER, M., WAGNER, D. E., OWEN, J. H. & REDDIEN, P. W. 2013.
817 Muscle cells provide instructions for planarian regeneration. *Cell Rep,* 4**,** 633-41.
818 YEBRA, M., MONTGOMERY, A. M., DIAFERIA, G. R., KAIDO, T., SILLETTI, S., PEREZ,
819 B., JUST, M. L., HILDBRAND, S., HURFORD, R., FLORKIEWICZ, E., TESSIER-

LAVIGNE, M. & CIRULLI, V. 2003. Recognition of the neural chemoattractant Netrin-1 by integrins alpha6beta4 and alpha3beta1 regulates epithelial cell adhesion and migration. *Dev Cell,* 5**,** 695-707.

ZENG, A., LI, H., GUO, L., GAO, X., MCKINNEY, S., WANG, Y., YU, Z., PARK, J., SEMERAD, C., ROSS, E., CHENG, L. C., DAVIES, E., LEI, K., WANG, W., PERERA, A., HALL, K., PEAK, A., BOX, A. & SANCHEZ ALVARADO, A. 2018. Prospectively Isolated Tetraspanin(+) Neoblasts Are Adult Pluripotent Stem Cells Underlying Planaria Regeneration. *Cell,* 173**,** 1593-1608 e20.

Figure 1

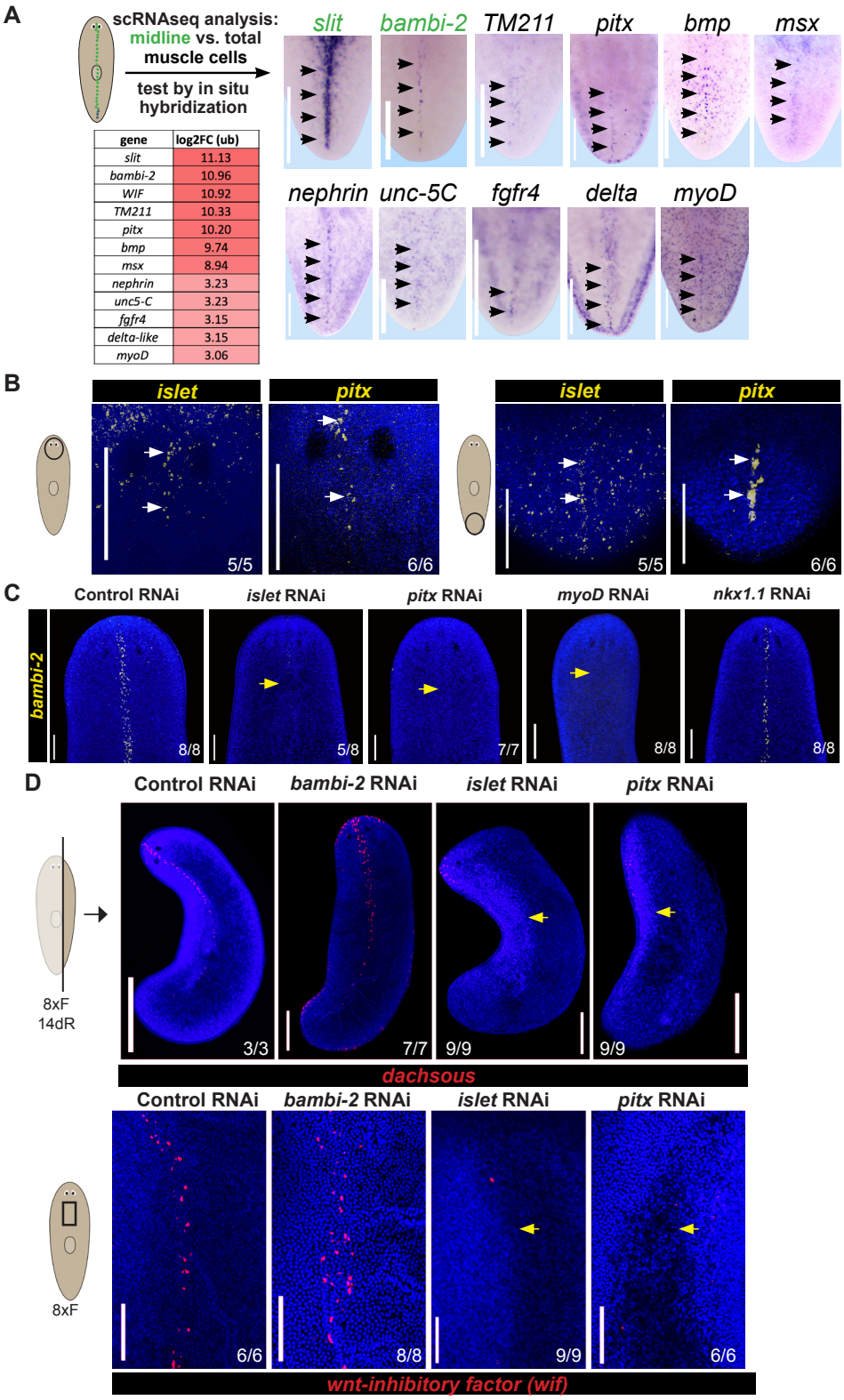

gene	log2FC (ub)
slit	11.13
bambi-2	10.96
WIF	10.92
TM211	10.33
pitx	10.20
bmp	9.74
msx	8.94
nephrin	3.23
unc5-C	3.23
fgfr4	3.15
delta-like	3.15
myoD	3.06

Figure 2

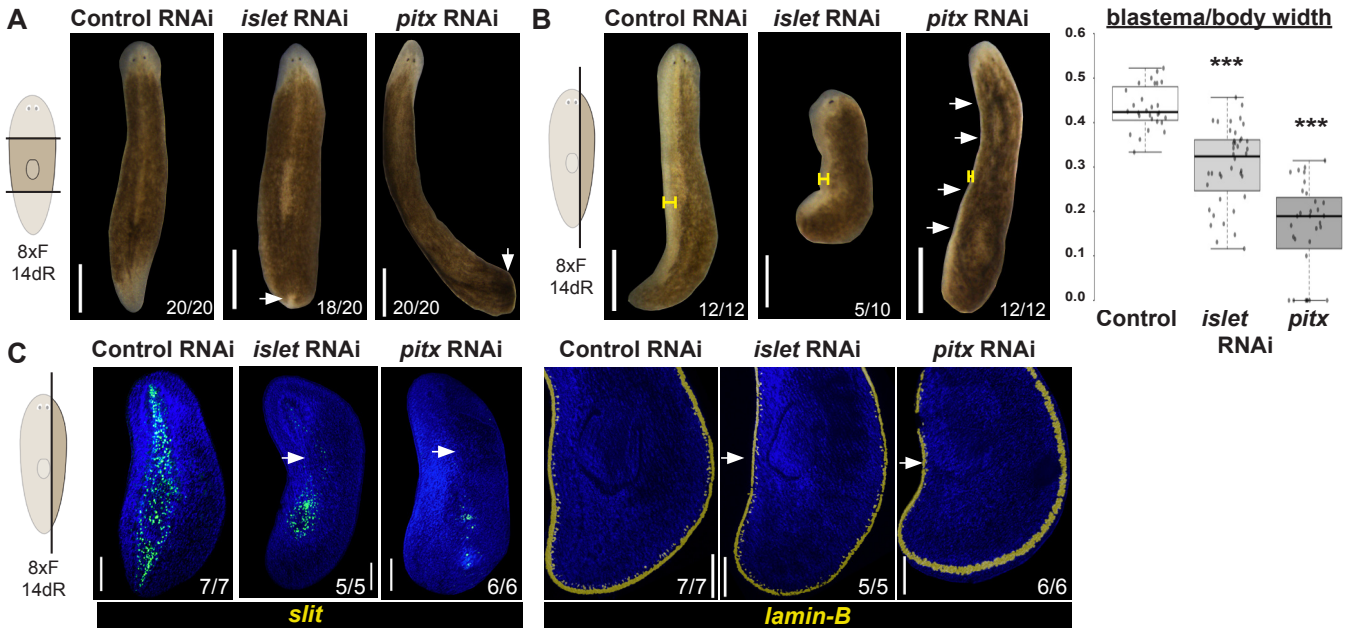
A
Control RNAi
islet RNAi
pitx RNAi
8xF
14dR
20/20
18/20
20/20
B
Control RNAi
islet RNAi
pitx RNAi
8xF
14dR
12/12
5/10
12/12
blastema/body width
0.6
0.5
0.4
0.3
0.2
0.1
0.0
***
***
Control
islet RNAi
pitx
C
Control RNAi
islet RNAi
pitx RNAi
8xF
14dR
7/7
5/5
6/6
slit
Control RNAi
islet RNAi
pitx RNAi
7/7
5/5
6/6
lamin-B

Figure 3

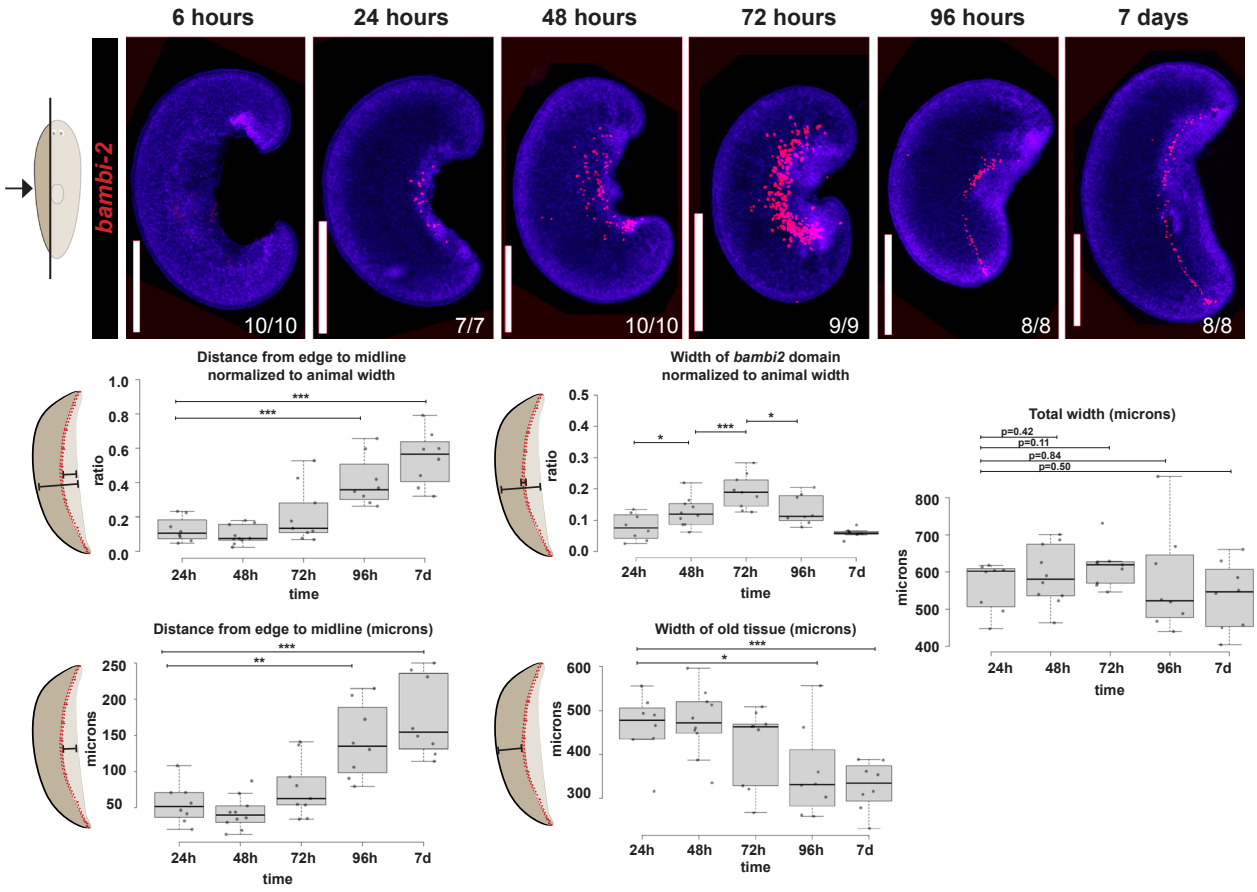
6 hours
24 hours
48 hours
72 hours
96 hours
7 days
bambi-2
10/10
7/7
10/10
9/9
8/8
8/8
Distance from edge to midline normalized to animal width
ratio
time
Width of bambi2 domain normalized to animal width
ratio
time
Total width (microns)
p=0.42
p=0.11
p=0.84
p=0.50
microns
time
Distance from edge to midline (microns)
microns
time
Width of old tissue (microns)
microns
time
24h
48h
72h
96h
7d

Figure 4

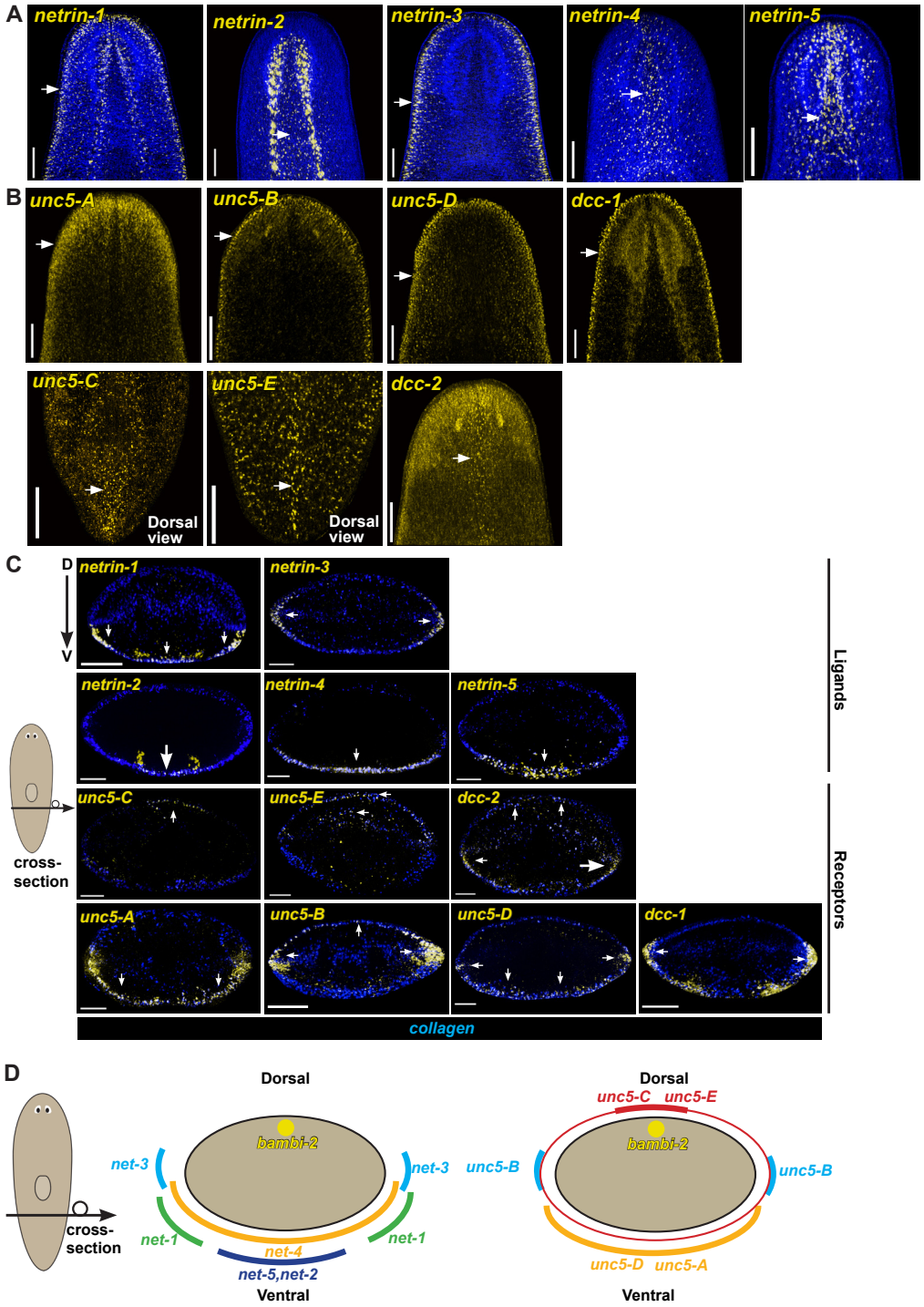
A
netrin-1
netrin-2
netrin-3
netrin-4
netrin-5
B
unc5-A
unc5-B
unc5-D
dcc-1
unc5-C
unc5-E
dcc-2
Dorsal view
Dorsal view
C
D
V
netrin-1
netrin-3
netrin-2
netrin-4
netrin-5
unc5-C
unc5-E
dcc-2
unc5-A
unc5-B
unc5-D
dcc-1
cross-section
Ligands
Receptors
collagen
D
cross-section
Dorsal
bambi-2
net-3
net-3
net-1
net-1
net-4
net-5,net-2
Ventral
Dorsal
unc5-C
unc5-E
bambi-2
unc5-B
unc5-B
unc5-D
unc5-A
Ventral

Figure 5

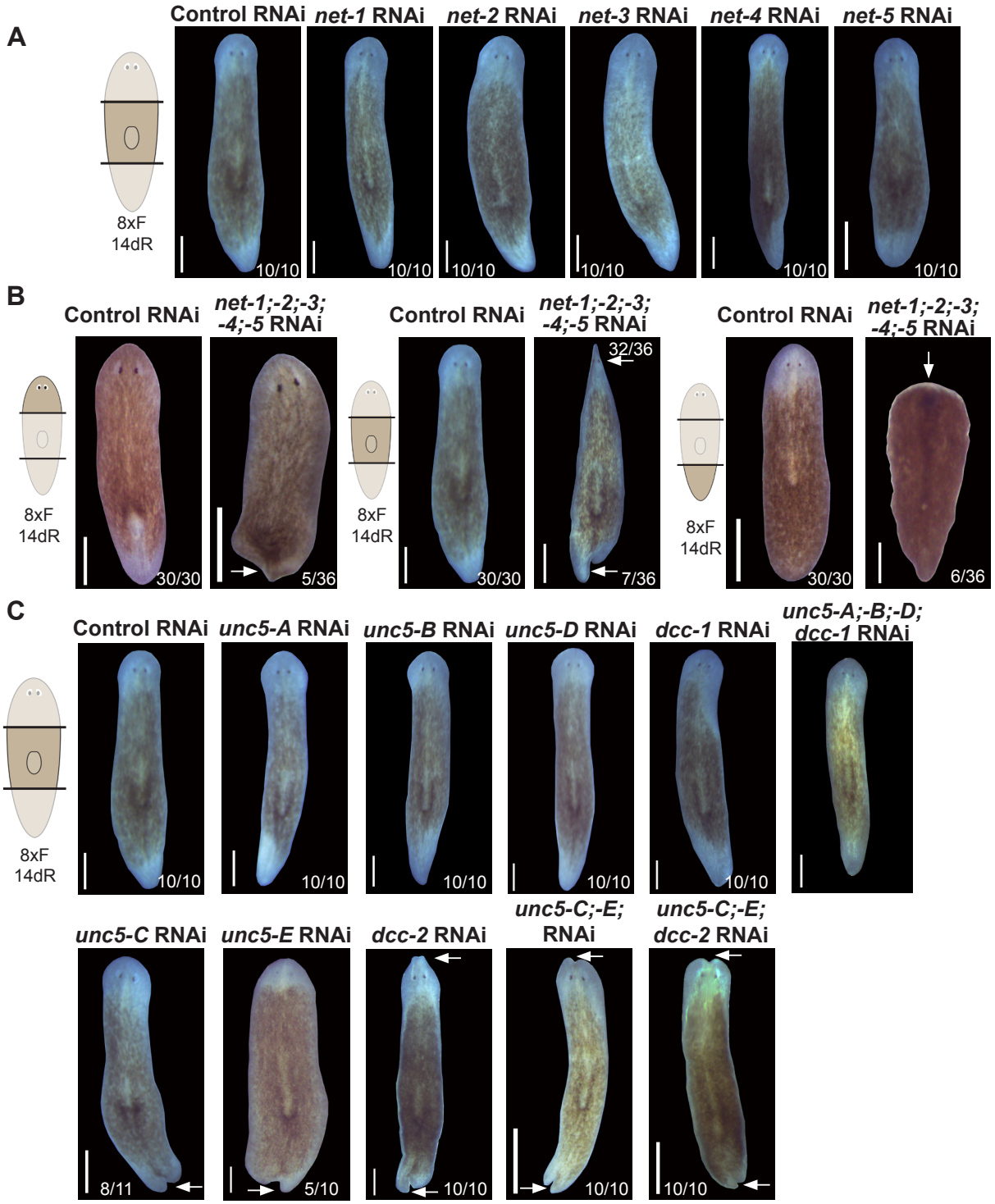
A
Control RNAi
net-1 RNAi
net-2 RNAi
net-3 RNAi
net-4 RNAi
net-5 RNAi
8xF
14dR
10/10
10/10
10/10
10/10
10/10
10/10
B
Control RNAi
net-1;-2;-3;
-4;-5 RNAi
8xF
14dR
30/30
5/36
32/36
7/36
6/36
C
Control RNAi
unc5-A RNAi
unc5-B RNAi
unc5-D RNAi
dcc-1 RNAi
unc5-A;-B;-D;
dcc-1 RNAi
10/10
unc5-C RNAi
unc5-E RNAi
dcc-2 RNAi
unc5-C;-E;
RNAi
unc5-C;-E;
dcc-2 RNAi
8/11
5/10
10/10

Figure 6

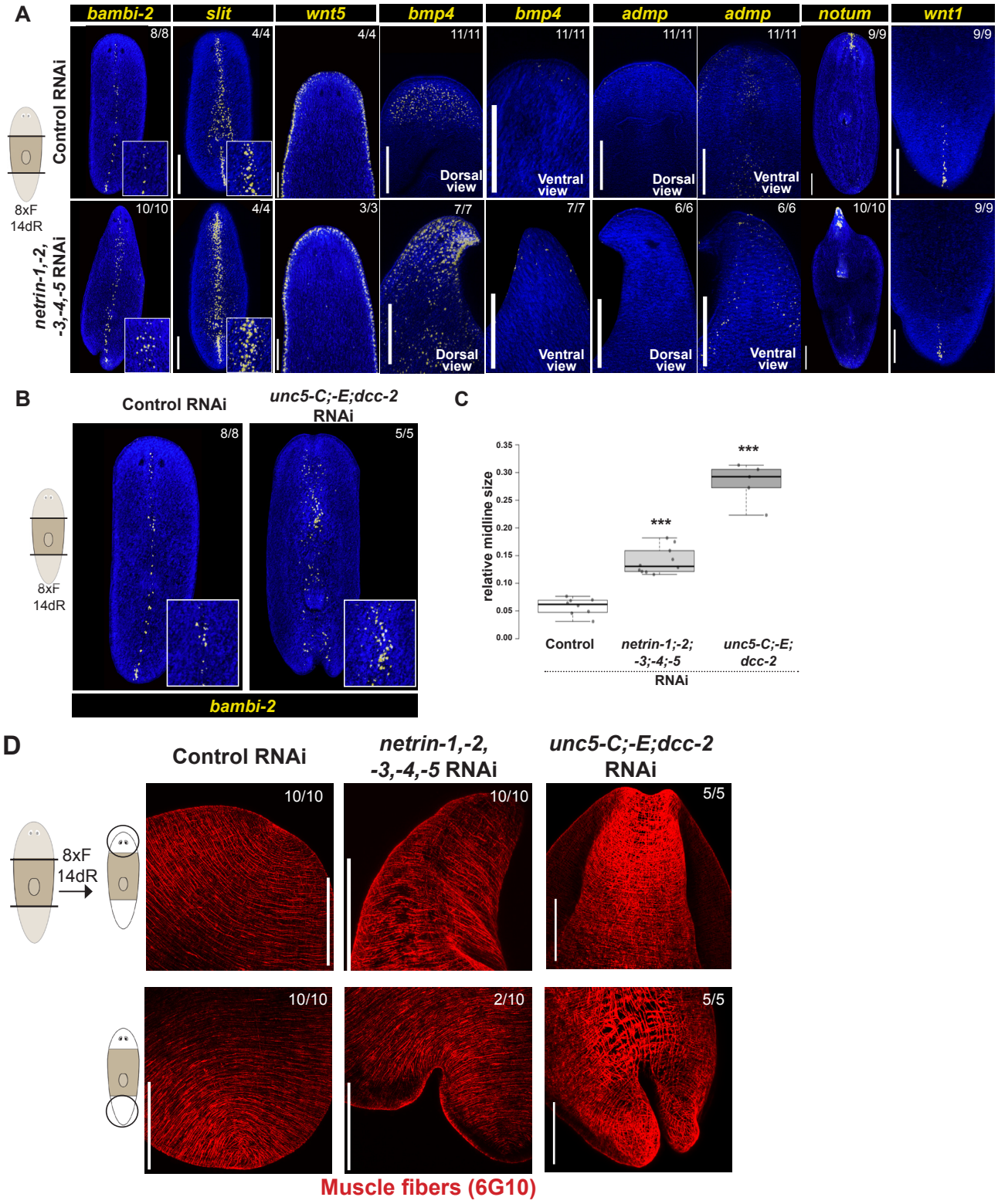
A
bambi-2
slit
wnt5
bmp4
bmp4
admp
admp
notum
wnt1
Control RNAi
netrin-1,-2, -3,-4,-5 RNAi
8xF
14dR
8/8
4/4
4/4
11/11
11/11
11/11
11/11
9/9
9/9
10/10
4/4
3/3
7/7
7/7
6/6
6/6
10/10
9/9
Dorsal view
Ventral view
B
Control RNAi
unc5-C;-E;dcc-2 RNAi
8/8
5/5
bambi-2
C
relative midline size
0.35
0.30
0.25
0.20
0.15
0.10
0.05
0.00
***
***
Control
netrin-1;-2; -3;-4;-5
unc5-C;-E; dcc-2
RNAi
D
Control RNAi
netrin-1,-2, -3,-4,-5 RNAi
unc5-C;-E;dcc-2 RNAi
10/10
10/10
5/5
10/10
2/10
5/5
Muscle fibers (6G10)

Figure 7

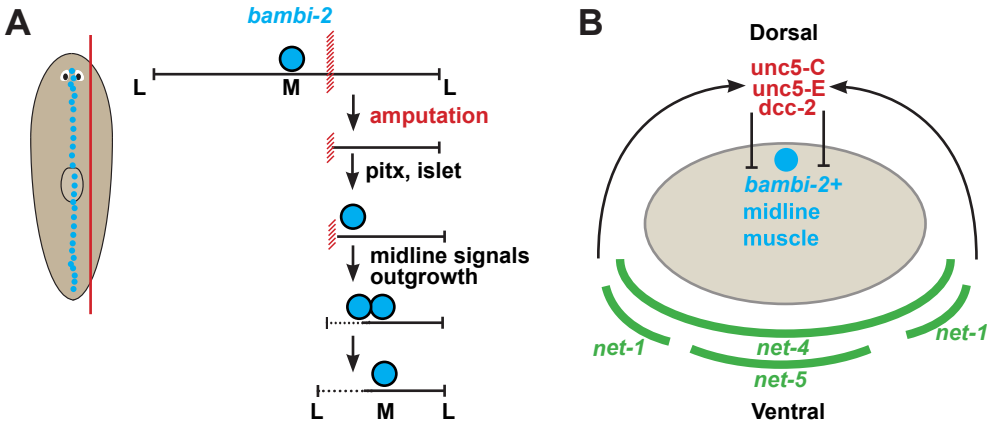
A
bambi-2
L
M
L
amputation
pitx, islet
midline signals
outgrowth
L
M
L
B
Dorsal
unc5-C
unc5-E
dcc-2
bambi-2+
midline
muscle
net-1
net-4
net-1
net-5
Ventral

Figure S1

A

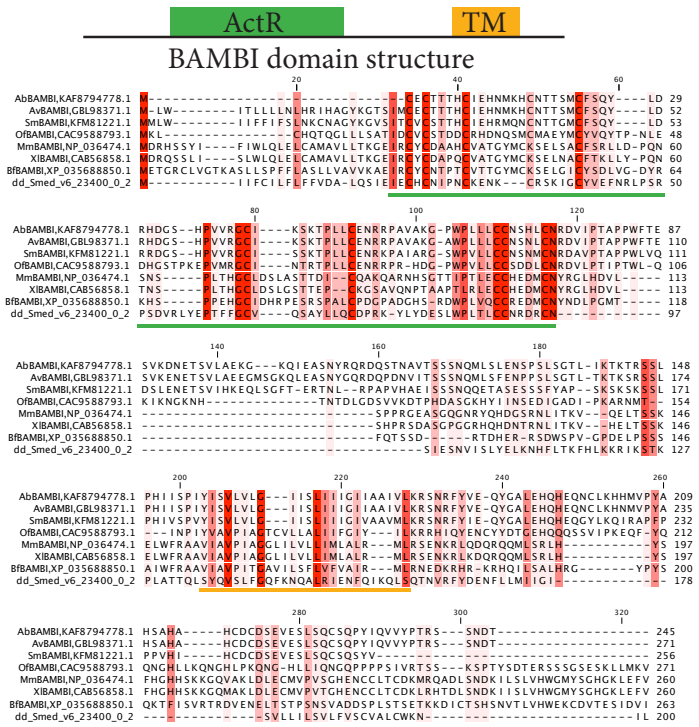
ActR
TM
BAMBI domain structure
AbBAMBI,KAF8794778.1
AvBAMBI,GBL98371.1
SmBAMBI,KFM81221.1
OfBAMBI,CAC9588793.1
MmBAMBI,NP_036474.1
XlBAMBI,CAB56858.1
BfBAMBI,XP_035688850.1
dd_Smed_v6_23400_0_2

B

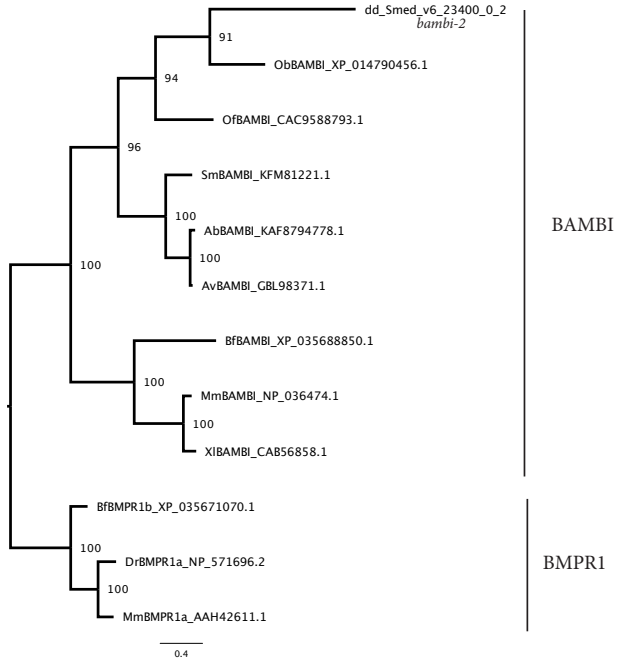
dd_Smed_v6_23400_0_2
bambi-2
ObBAMBI_XP_014790456.1
OfBAMBI_CAC9588793.1
SmBAMBI_KFM81221.1
AbBAMBI_KAF8794778.1
AvBAMBI_GBL98371.1
BfBAMBI_XP_035688850.1
MmBAMBI_NP_036474.1
XlBAMBI_CAB56858.1
BfBMPR1b_XP_035671070.1
DrBMPR1a_NP_571696.2
MmBMPR1a_AAH42611.1
BAMBI
BMPR1
0.4

Figure S2

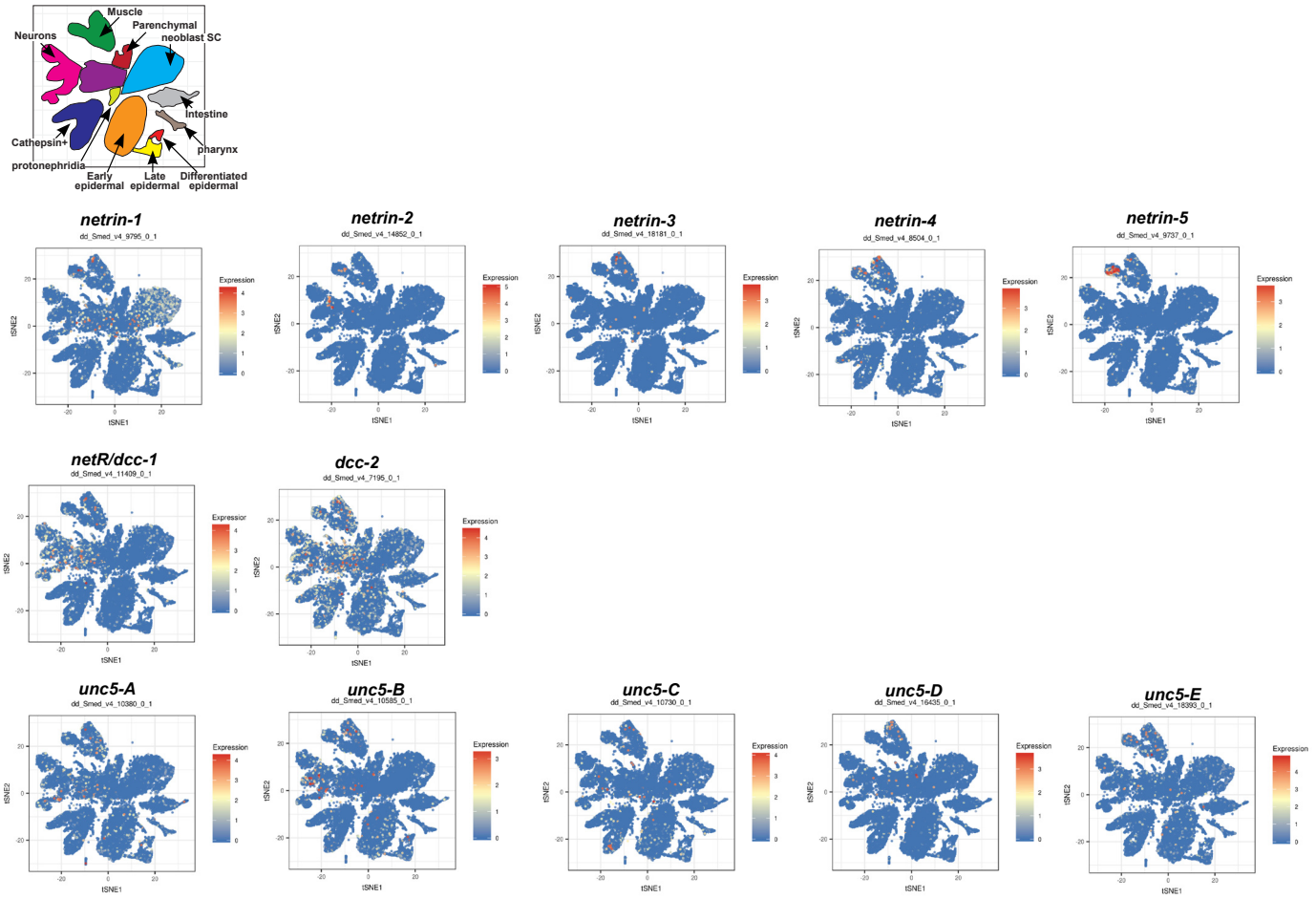
Muscle
Parenchymal
Neurons
neoblast SC
Intestine
Cathepsin+
pharynx
protonephridia
Early epidermal
Late epidermal
Differentiated epidermal
netrin-1
dd_Smed_v4_9795_0_1
netrin-2
dd_Smed_v4_14852_0_1
netrin-3
dd_Smed_v4_18181_0_1
netrin-4
dd_Smed_v4_8504_0_1
netrin-5
dd_Smed_v4_9737_0_1
netR/dcc-1
dd_Smed_v4_11409_0_1
dcc-2
dd_Smed_v4_7195_0_1
unc5-A
dd_Smed_v4_10380_0_1
unc5-B
dd_Smed_v4_10585_0_1
unc5-C
dd_Smed_v4_10730_0_1
unc5-D
dd_Smed_v4_16435_0_1
unc5-E
dd_Smed_v4_18393_0_1
Expression
tSNE1
tSNE2

Figure S3

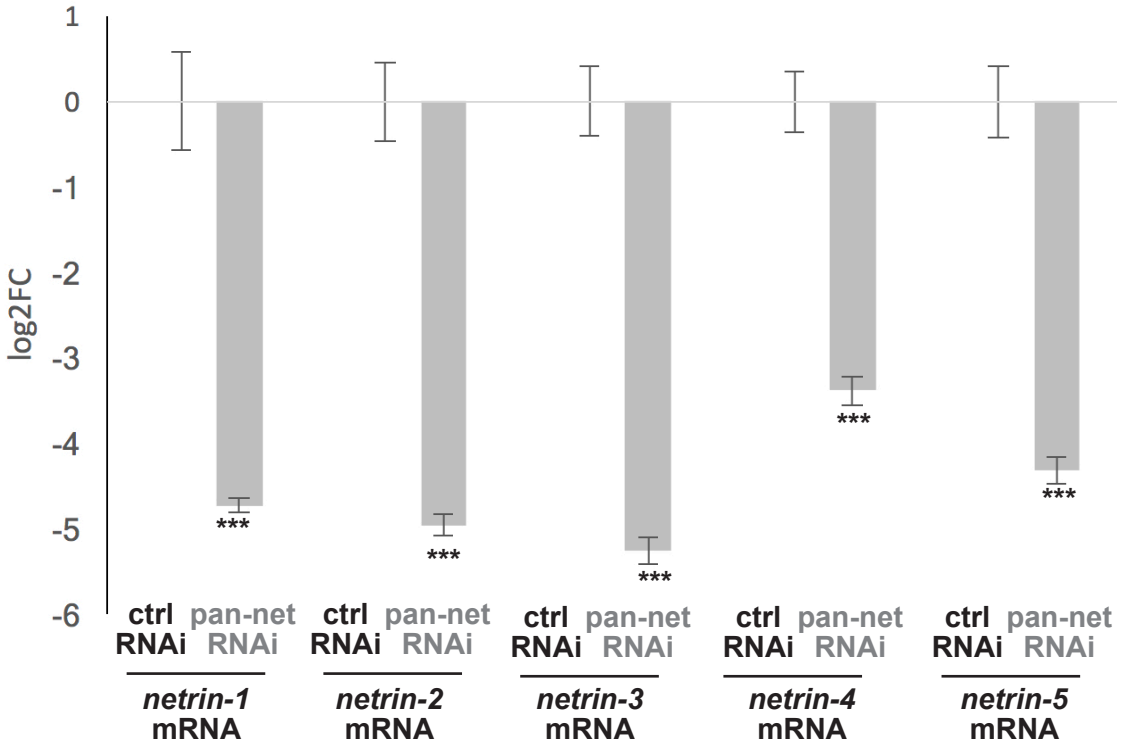
1
0
-1
-2
-3
-4
-5
-6
log2FC
***
***
***
***
***
ctrl RNAi
pan-net RNAi
netrin-1 mRNA
netrin-2 mRNA
netrin-3 mRNA
netrin-4 mRNA
netrin-5 mRNA

Figure S4

A

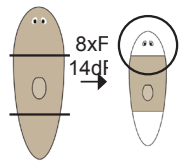

Score for pointy blastema

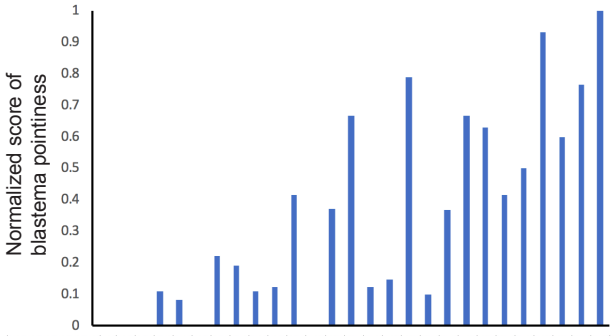

netrin-1	-	+	+	+	+	-	-	-	-	-	-	+	+	+	+	+	+	-	-	-	-	+	+	+	+	-	+
netrin-2	-	+	-	-	-	-	+	+	+	-	-	-	+	+	+	-	-	-	+	+	+	-	+	+	+	-	+	+
netrin-3	-	-	+	-	-	-	+	-	-	+	+	-	+	-	-	+	+	-	+	+	-	+	+	+	-	+	+	+
netrin-4	-	-	-	+	-	-	+	-	+	-	+	-	+	-	+	-	+	+	-	+	-	+	+	+	-	+	+	+
netrin-5	-	-	-	-	-	+	-	-	+	-	+	+	-	-	+	-	+	+	-	+	+	+	-	+	+	+	+	+

RNAi condition

8xF
14dR

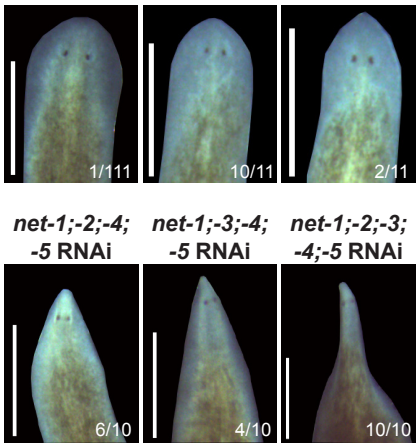

B

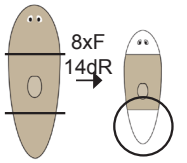

Score for indented blastema

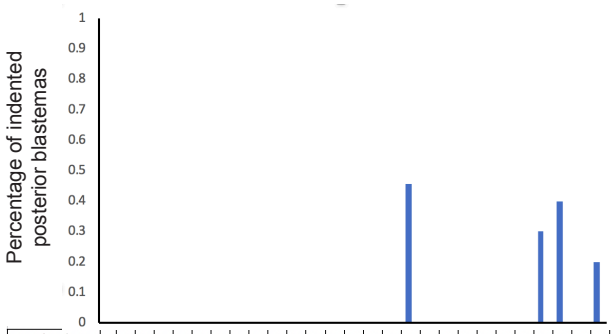

netrin-1	-	+	+	+	+	-	-	-	-	-	-	+	+	+	+	+	+	-	-	-	-	+	+	+	+	-	+
netrin-2	-	+	-	-	-	-	+	+	+	-	-	-	+	+	+	-	-	-	+	+	+	-	+	+	+	-	+	+
netrin-3	-	-	+	-	-	+	-	-	+	+	-	+	-	-	+	+	-	+	+	+	-	+	+	+	-	+	+	+
netrin-4	-	-	-	+	-	-	+	-	+	-	+	-	+	-	+	-	+	+	-	+	+	+	-	+	+	+	+	+
netrin-5	-	-	-	-	+	-	-	+	-	+	+	-	-	+	-	+	+	-	+	+	+	-	+	+	+	+	+	+

RNAi condition

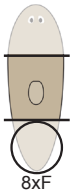

8xF
14dR

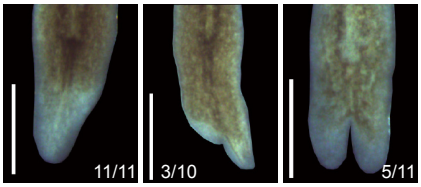

Figure S5

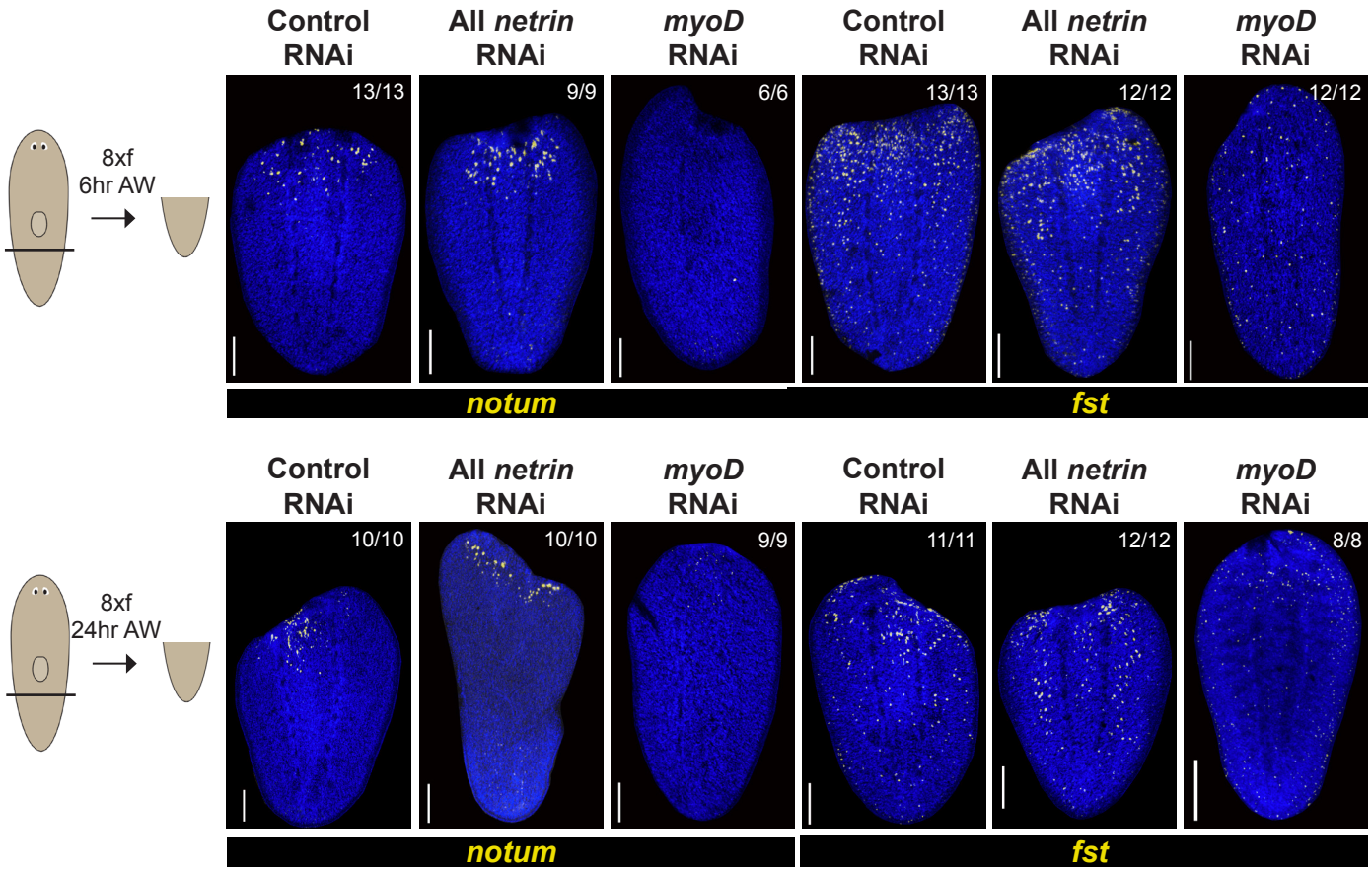
Control RNAi
All netrin RNAi
myoD RNAi
Control RNAi
All netrin RNAi
myoD RNAi
8xf
6hr AW
13/13
9/9
6/6
13/13
12/12
12/12
notum
fst
Control RNAi
All netrin RNAi
myoD RNAi
Control RNAi
All netrin RNAi
myoD RNAi
8xf
24hr AW
10/10
10/10
9/9
11/11
12/12
8/8
notum
fst